Seismological Research Letters

ESMpro: a proposal for improved data management for the Engineering Strong Motion database (ESM)

--Manuscript Draft--

Manuscript Number:	SRL-D-22-00246R3
Full Title:	ESMpro: a proposal for improved data management for the Engineering Strong Motion database (ESM)
Article Type:	Electronic Seismologist
Corresponding Author:	Claudia Mascandola INGV Milano, ITALY
Corresponding Author Secondary Information:	
Corresponding Author's Institution:	INGV
Corresponding Author's Secondary Institution:	
First Author:	Claudia Mascandola
First Author Secondary Information:	
Order of Authors:	Claudia Mascandola
	Maria D’Amico
	Emiliano Russo
	Lucia Luzi
Order of Authors Secondary Information:	
Manuscript Region of Origin:	ITALY
Suggested Reviewers:	Carlo Virgilio Cauzzi ETH carlo.cauzzi@sed.ethz.ch Expert in seismic network operations and products; seismic data collection, curation and dissemination. He coordinates observatories & research facilities for European seismology. He deals with strong-motion seismology, earthquake engineering and digital signal processing.
	Eric Thompson USGS He developed the USGS automated ground motion processing software. He is expert in digital signal processing; seismic network operations and products; seismic data collection, curation and dissemination.
	John Douglas Senior Lecturer, University of Strathclyde john.douglas@strath.ac.uk He has expertise in strong-motion databases and in processing of strong-motion records.

ESMpro: a proposal for improved data management for the Engineering Strong Motion database (*ESM*)

Claudia Mascandola*(1), Maria D'Amico(1), Emiliano Russo(1) Lucia Luzi (1)

(1) Istituto Nazionale di Geofisica e Vulcanologia, Via Alfonso Corti 12, 20133, Milan

* **Corresponding author**

Claudia Mascandola

Address: Via Alfonso Corti 12, 20133, Milan

Phone: +39 02 23699 284

e-mail: claudia.mascandola@ingv.it

Abstract

The strategy for data processing in the Engineering Strong-Motion database (ESM) is to disseminate only manually revised data to ensure the highest quality. However, manual processing is no longer sustainable, due to the ever-increasing rate of digital earthquake records, from global, regional and national seismic networks, and a new framework for strong-motion data processing is required, so that records are automatically processed and the human revision is restricted to selected significant records. To this end, we present ESMpro, a modular Python software for a renewed processing framework of ESM. The software is available in a stand-alone Beta version, to facilitate testing and sharing among the scientific community.

ESMpro provides automatic settings for waveform trimming and filtering, along with the automatic recognition of poor-quality data and multiple events. ESMpro allows classifying each record in different quality classes to reduce manual revision on a subset of the incoming data. ESMpro also allows handling different processing techniques in a modular and flexible structure to facilitate the implementation of new or alternative algorithms and file formats. The testing performed on the ESM database results in a good correspondence between the automatic and manual data processing, supporting the migration towards fully automatic procedures for massive data processing.

Introduction

Strong-motion records and open access to strong-motion data repositories are fundamental to seismology, earthquake engineering science and practice. However, to ensure a proper use of these records, a reliable strong-motion data processing is necessary to disseminate good-quality waveforms free from signal distortion (e.g., noisy band frequency, flatline channels, spurious spikes, early termination during coda, multiple baselines). The strong-motion data quality control is a challenging task, which becomes more important in the case of large strong-motion data sets. In addition, given the high growth rate of earthquake records from global, regional, and national seismic networks, it is vital to manage the storage of strong-motion databases, which potentially could contain a huge number of seismic waveforms.

In the last few years, numerous papers have focused on the issue of strong-motion data processing and quality control procedures. In many cases, schemes for data processing procedures (e.g., Boore, 2005; Boore and Bommer, 2005; Akkar and Boore, 2009; Massa et al., 2010; Pacor, Paolucci, Ameri, et al., 2011; Pacor, Paolucci, Luzi, et al., 2011; Paolucci et al., 2011; Boore et al., 2012; Puglia et al., 2018), open-source tools (e.g., Weber et al., 2007; Hosseini and Sigloch, 2017; Jones et al., 2017; Kalkan and Stephens, 2017; Hearne et al., 2019; Zaccarelli et al., 2019; Petersen et al. 2019), and commercial software (e.g., Papazafeiropoulos and Plevris, 2018) for strong-motion data analyses are addressed to off-line seismic waveforms datasets, relevant seismic sequences (e.g., Massa et al., 2016; Cara et al., 2019; Rekoske et al., 2020), or to the compilation of flat-files for engineering applications (e.g., Akkar et al., 2010; Luzi et al., 2016; Bindi et al., 2018; Lanzano et al., 2019; Bahrampouri et al., 2021). Moreover, machine learning models for the automatic detection of anomalies on data and metadata (Zaccarelli et al., 2021; Kleckner et al., 2021) or automated quality screening of ground motion records from small magnitude earthquakes (Bellagamba et al. 2019) have also been developed. Several stand-alone software packages are also available for the quality control of seismic data (Ringler et al., 2015; Sharer et al., 2017; Casey et al., 2018; Hearne et al., 2019; Aur et al., 2021).

There are two main strategies to disseminate strong-motion records: the first is to assure a rapid open access to automatically processed waveforms and related metadata (e.g., Massa et al., 2014; Cauzzi et al., 2016; Jones et al., 2017; Kalkan and Stephens, 2017; Massa et al., 2022); the second is to provide strong-motion data reviewed by experts with some delay after an earthquake occurrence. In this case, the main archive to disseminate good quality processed waveforms for the European-Mediterranean region is the Engineering Strong-Motion Database (ESM, see Data and Resources).

ESM is developed under the umbrella of ORFEUS (Observatories and Research Facilities for European Seismology, see Data and Resources), which is a pillar of the Thematic Core Service for Seismology (Haslinger et al., 2022) of EPOS (European Plate Observing System, see Data and Resources), a multidisciplinary, distributed research infrastructure that facilitates the integrated use of data, data products, and facilities from the solid Earth science community in Europe. The ESM database was designed for a large variety of stakeholders (seismologists, earthquake engineers, students, and professionals) to access earthquake waveforms of engineering interest ($M \geq 4.0$), mainly recorded in the EuroMediterranean region since 1969, with the associated metadata (e.g., Luzi et al., 2016; Lanzano et al., 2021).

The ESM database is daily updated and currently contains more than 7,000 events, more than 11,000 stations, and about 80,000 waveforms (last accessed June 2022). The geographic distribution of events is shown in Figure 1a. Most events are located in the EuroMediterranean region, in particular in Greece, Turkey and Italy, but also all over the world, due to European data providers operating seismic networks in other countries. The geographic distribution of the stations is displayed in Figure 1b, showing a high concentration in Italy, Turkey, Taiwan, Greece, Switzerland and France. As regards the waveforms archived in ESM, the magnitude-frequency distribution (Figure 2a) shows a large number of records in the medium-magnitude (4-5), high-distance (100-200 km) ranges. The increasing rate of digital earthquake records, from global, regional, and national seismic networks is evident in Figure 2b, showing the large number of waveforms per year relative to the last two decades. In particular, during seismic sequences like the one in Central Italy in 2016 (e.g., Luzi et al., 2017), the growth rate of ground-motion data can increase exponentially, complicating the manual revision soon after the earthquake occurrence.

In this work, we describe the main features of ESMpro, the Python software (see Data and Resources) developed to drastically reduce human intervention, related to the increasing availability of digital strong-motion data. The main features of ESMpro are: 1) quality check of unprocessed waveforms to identify records with priority for manual revision; 2) data processing with different methods; and 3) object-oriented design to facilitate the implementation of further algorithms and tools (e.g., data conversion or detection of near-source impulsive signals). The performance of ESMpro is tested by comparing the waveforms automatically processed and about 70,000 manually-revised, openly available waveforms in the ESM database.

ESMpro has been developed to be fully integrated with the existing ESM infrastructure. The software package is delivered as a stand-alone Beta version developed in Python 3.0 (see Data and Resources).

On improving the ESM data management

The workflow for an improved ESM data management strategy (Figure 3) can be summarized in: (1) pre-processing phase, which includes data harvesting, quality check, setting for automatic processing; and (2) processing phase, which implies automatic processing and manual revision.

Data Harvesting

After the occurrence of seismic events with magnitude threshold 4.0, a signal windowing procedure is applied to continuous acceleration streams, available at the European Integrated Data Archive (EIDA, see Data and Resources) and the Incorporated Research

Institutions for Seismology (IRIS, see Data and Resources) webservices. Time series in digital counts are converted into physical units (cm/s^2) after simple gain correction, and the mean acceleration is removed from the signal. ESM also includes off-line data from some data centers that are not EIDA nodes, such as the Italian Civil Protection Department (network code IT). The ESM waveforms are stored in a file system, exploiting the capacity of the Adaptable Standard Data Format (ASDF, Krischer et al., 2016) to include, in a single file object, time series (uncorrected and corrected acceleration, velocity, displacement), response spectra (acceleration and displacement), and related metadata. Event, station, and waveform metadata, along with ground motion intensity measures, are stored in a PostgreSQL relational database.

Quality check

The quality check in the pre-processing phase classifies the waveforms according to: 1) input data requirements; 2) signal-to-noise ratio in time domain (SNR_T); and 3) additional features (Table 1). Some preliminary checks ensure that all mandatory requirements to run ESMpro are fulfilled (e.g., wrong format, noncompliant mandatory metadata, dead or empty channels; Figure 3). After that, noise and signal windows should be identified to compute the SNR_T. However, in some cases the pre-processing algorithm could fail during waveform trimming (Figure 4a) or picking the P and S wave arrivals (Figure 4b). In these cases, the SNR_T cannot be computed; otherwise, we compute the SNR_T from 4s noise and signal windows as described in Appendix S1.

The distribution of the SNR_T values of the ESM waveforms (Figure 5) shows that most data have a high Signal-to-Noise ratio, with an average of 14.3 dB (Figure 4c) and a standard deviation of 12.5 dB. Based on this distribution, we decided to set an empirical threshold of 6 dB (Figure 4d) to identify the noisy traces. A few data show extremely high SNR_T ($\geq$ 60 dB;

red circle in Figure 5) that are often artifacts related to instrumental issues or bad signal acquisitions (Figure 4e).

When SNR_T ranges between 6-60 dB, the record goes to the additional checks reported in Table 1. Since these are not mutually exclusive, they are addressed in sequential order. Firstly, we check for extreme Peak Ground Acceleration (PGA) values. The PGA is considered suspect when it is greater than 2g on at least one of the three components (Figure 4f). Secondly, we check for suspected acceleration components: if one horizontal component is more than twice the other, based on PGA or Root Mean Square (RMS) values (Figure 4g), the data should be manually revised because one component may be biased. The same check is performed on the vertical component, considering a threshold of three times the horizontal ones. Indeed, the horizontal components have an average PGA ratio of 0.9 and they are about 1.6 times the vertical one (Figure S1): the thresholds for the amplitude checking are twice these ratios. Subsequently, we check the reliability of the theoretical P wave arrival considering the lag with the 5% of the Normalized Arias Intensity (Arias, 1970). A significant lag (Figure 4h) may cause an improper trimming around the target event (see Appendix S2). After that, we check the occurrence of multiple events by applying a trigger algorithm (Recursive STA/LTA in Obspy, see Data and Resources). If more than one trigger occurs inside the significant duration (i.e., $D_{5\text{-}95}$: time span between 5% and 95% of the Normalized Arias Intensity; Arias 1970) of the ground motion, the waveform is flagged as multiple events (Figure 4i). The target event is identified by the trigger closest to the theoretical P wave arrival. Finally, we check for records characterized by a usable frequency bandwidth of Fourier spectrum in the interval 0.4–20 Hz (i.e., a low-cut frequency of the bandpass filter greater than 0.4 Hz or a high-cut frequency of the bandpass filter lower than 20 Hz). Indeed, the good-quality waveforms in ESM always preserve the Fourier Amplitude Spectrum in this frequency range (Lanzano et al., 2019). A restricted frequency passband may be critical for the usability of the response spectral values

(Ancheta et al., 2014; Douglas and Boore, 2011) and it is usually related to a low signal-to-noise ratio or to disturbances on one ground-motion component. Figure 4j shows an example due to a bad signal acquisition on the North-South component. In this case, the disturbances also affect the automatic picking. When the 4s noise window for the SNR_T computation cannot be selected before the P-wave arrival, the noise window is taken starting from the end of the trace (Figure 4j).

Based on the applied quality checks, we propose the following waveform classification (Figure 6):

- A - records with SNR_T in the range 6-60 dB;
- B - records with SNR_T in the range 6-60 dB affected by some additional features (Table 1);
- C - records with $SNR_T \leq$ 6dB, or $SNR_T \geq$ 60dB affected by signal distortions;
- D - records that caused unexpected errors while computing SNR_T or featured by improper input data/metadata.

These four quality classes can support decisions on automatic and manual processing in ESM. Only records in A and B classes should be automatically processed and a higher priority for manual revision is suggested for B and D classes (Figure 6).

Data Processing and Settings

Uncorrected acceleration signals are automatically processed using two alternative methods. The first one, PAO11 (Paolucci et al., 2011; Figure 3), is the default scheme and it is always applied to ensure full compatibility between acceleration and velocity or displacement, obtained by single and double integration of processed accelerations, respectively (Puglia et al., 2018). The workflow of PAO11 is essentially based on a first order linear detrending, cosine taper with for a fixed percentage of the signal length (both at the beginning and the end of the trace), and 2nd order acausal time-domain Butterworth bandpass filter. Zero-pads, in particular, are added at the beginning and end of the signal, before the acausal filter is applied (Boore, 2005). However, this may pose several problems when using the corrected accelerograms; therefore the original time-scale is re-established after filtering, whenever feasible. This is done by removing the zero-pads and by ensuring that the subsequent tapering of velocity and displacement will produce time histories starting from zero initial conditions. The second one, eBASCO (Schiappapietra et al., 2021; Figure 3), is specifically tailored to process near source data featuring fling-step. Differently from PAO11, eBASCO is applied only to near-source records (Pacor et al., 2018; D'Amico et al., 2018; Sgobba et al., 2021). It is based on a piecewise linear detrend of the velocity signal, a cosine taper applied only at the beginning of the trace (for a fixed percentage of the signal length), and 2nd order acausal time-domain Butterworth low-pass filter (Schiappapietra et al., 2021).

Among the processing settings required by both methods, the waveform trimming and the Butterworth bandpass filter often require the visual inspection of time series and Fourier spectra. Indeed, the raw data retrieved from continuous streams (considering the event metadata) are often featured by long noise windows before or after the event, which may be annoying for engineering and practitioners that adopt these waveforms in several applications. The refinement of the waveform trimming around the target event can be automatically performed by applying a trigger algorithm (Recursive STA/LTA in Obspy, see Data and Resources), along with the theoretical P wave arrival to discard false triggers and select the correct one in case of multiple events. The procedure for the automatic trimming is described in Appendix S2.

A further improvement for the automatic settings regards the cut-off frequencies of the bandpass filter: the low-cut (lc) and high-cut (hc) frequencies (Paolucci et al. 2011; Puglia et al. 2018) are the most important parameters to set. An improper bandpass filtering can alter the frequency content of the signal with significant impact on the representativeness of the recorded earthquake and, consequently, on the calibration of ground motion models. To set the cut-off frequencies of the bandpass filter we apply the classical signal-to-noise ratio in frequency domain (SNR_F). The automatic picking of P-wave arrivals divides the pre-event noise from the signal. The noise and signal windows have the same length, which is constrained by the duration of available pre-event noise (Figure 7a). The Fast Fourier Transform on the signal (FFT_S) and noise (FFT_N) windows is computed and smoothed with a Konno-Ohmachi smoothing (Figure 7b). The cut-off frequencies of the bandpass filter are detected when the SNR_F [$(FFT_S$-$FFT_N)/FFT_N$] exceeds 2 (Figure 7c). The method is described in detail in Appendix S3. If the SNR_F curve is always above the predefined threshold, the lc frequency depends on magnitude ranges (Puglia et al., 2018). On the contrary, the hc frequency is set at 40 Hz to avoid anthropic and instrumental noise often observed at higher frequencies (Trnkoczy et al., 2012).

Testing

The ESMpro improvement related to quality check and automatic settings are tested on ~70,000 records in ESM. These records, already revised by ESM operators as good (~45,000) or bad (~22,000) quality waveforms, can be adopted to test the effectiveness of ESMpro in replacing manual processing and reducing time for human intervention. Figure 8 shows the results of this test. Figure 8a shows that most of the good quality records in ESM are classified in the best quality class by ESMpro (class A). The remaining records are mainly classified in class B, due to the restricted frequency passband or anomalous amplitudes on one component; in the minority for more events detected on the same trace or for unreliable P-wave arrivals.

Finally, most of the records classified in class C are close to the SNR_T threshold of 6 dB (Figure S2), with just a minor amount related to failing of automatic picking or trigger (Figure 8a).

In addition, Figure 8b shows that most of the bad quality data in ESM is classified in quality class C due to the signal-to-noise ratio; with just a minor amount related to the failing of automatic picking or trigger. The distribution of the remaining records is similar to the good quality dataset, with records mainly classified in class B, due to the restricted frequency passband or anomalous amplitudes on one component; in the minority for more events detected on the same trace, unreliable P-wave arrivals or for very few records with PGA > 2g. Also in this case, the records classified in A are close to the SNR_T threshold of 6 dB (Figure S2); whereas differently from the good quality dataset, here we have a few records in class D, mainly for the presence of one zero component (Figure 8b). The very limited occurrence of D classes indicates a proper input data organization inside the HDF5 container, with all the mandatory requirements fulfilled.

The automatic settings for waveform trimming (i.e., startime and endtime), along with those for the waveform filtering (i.e., lc and hc frequencies) are tested on the ESM good quality data. Figure 8c and 8d show the testing for the startime and endtime, respectively, plotting the residual time (i.e., automatic minus manual time) versus distance. The startime has an average residual close to zero (Figure 8c), whereas the endtime has a positive average residual (Figure 8d), which means that the ESMpro automatic trimming generally provides more samples after the signal window. This allows including the longer coda waves that may occur on the velocity or displacement time histories.

The same testing is performed on the frequencies of the bandpass filter. Since ESM provides the same cut-off frequencies for all the three ground-motion components, in the comparison between automatic and manual processing we consider the maximum lc and the mean hc detected by ESMpro on the three ground-motion components. Figure 8e and 8f show the testing for lc and hc frequencies respectively, evaluating the statistical distribution of residuals (i.e., automatic minus manual frequency). The lc residuals are mostly distributed around zero, with a coda toward positive values (Figure 8e), whereas the hc residuals are more variable, with a broader distribution centered toward negative values (Figure 8f). Overall, these results indicate a good correspondence between automatic and manual lc frequencies, whereas the correspondence on hc frequencies is not so good due to lower frequencies obtained from the signal-to-noise ratio. However, it is worth noting that the distribution of residuals is affected by the different approach adopted for the automatic setting of the cut-off frequencies. The manual cut-off frequencies are generally fairly stable around 0.1-0.2 Hz for lc, and around 30-50 Hz for hc, because they are set according to the magnitude value (Puglia et al., 2018) for lc, and fixed to 40 Hz for hc (Figure S3). These predefined values are not always modified after manual revision. On the contrary, the automatic frequencies are more variable according to the signal-to-noise ratio of each trace (Figure S3).

Finally, the automatic recognition of multiple events cannot be tested on the entire ESM dataset because this information was not stored in the database. To this end, we have prepared a specific testing dataset, where the recognition of multiple events is performed manually (Table S1). Overall, 184 good quality records and 95 bad quality records are visually inspected to check the occurrence of multiple events on the same trace. The automatic procedure is able to identify most of the multiple events recognized manually, even if some noisy records are erroneously identified as multiple events. As expected, this amount increases from 7% on the good quality data, to 29% on the bad quality data (Figure S4). The testing for automatic processing of these records (i.e., records with multiple events automatically detected) is reported in Figure 8c and 8d for waveform trimming, and in Figure 8e and 8f for waveform filtering. The results show the same distribution of the other ESM data, excluding systematic biases on these particular records.

Discussion and Conclusions

ESMpro is an ongoing project aimed at improving the data quality and management system of the Engineering Strong Motion database. Even though ESMpro has been developed to be fully integrated on the ESM infrastructure, a stand-alone Beta version of the software is available (see Data and Resource) to facilitate testing and sharing among the scientific community.

The pre-processing phase of ESMpro can be implemented at the beginning of the data processing pipeline of ESM, to flag peculiar issues (e.g., noisy records, multiple events, anomalous amplitudes, etc.) and assign a quality class to each record. The quality control helps the system maintenance of ESM, avoiding the data processing of low-quality records, thus preserving storage capacity. The automatic quality check introduced in ESMpro, along with the improvement of automatic settings for waveform trimming and filtering, will reduce time for manual revision, giving priority to some selected data and providing record-specific automatic settings. In addition, ESMpro allows treating strong-motion data with different processing techniques based on standard broadband waveform filtering or piece-wise linear detrending to preserve the low-frequency content of near-source records. The modular and flexible structure of ESMpro facilitates the implementation of further processing techniques and new alternative algorithms for automatic processing, including additional quality checks.

ESMpro presents similarities with gmprocess by Hearne et al. (2019), as both software were designed to provide a number of functions related to automatically parsing and processing earthquake ground motion data, building on top of the Obspy library (Krischer et al., 2015). However, ESMpro and gmprocess also present differences in motivation and philosophy. The former is developed to be fully integrated with the ESM database to save time for manual revision, keeping the same current data quality assurance; the latter is developed to facilitate the creation of ground-motion datasets with standardized processing algorithms.

ESMpro is not currently in production, but will go through a testing phase in a staging environment. In the next future, a renewed ESM web-processing frontend will be developed to include all the ESMpro improvements, as well as new functionalities to process stand-alone data (i.e., not stored in the ESM database) and to allow different input seismic data formats. Further improvements will be devoted to testing new algorithms for the automatic processing, having the unique possibility of having ∼70,000 ESM records, manually processed, as target for the automatic settings.

Data and Resources

A beta version of ESMpro, written in Python language (https://www.python.org), is available at: https://shake.mi.ingv.it/esmpro/. The Engineering Strong-Motion Database (ESM) was developed in the framework of the ORFEUS project, available at https://www.orfeus-eu.org/, which is one of the pillars of the EPOS Research Infrastructure, available at https://www.epos-eu.org/.

The webpage of the Engineering Strong Motion Database (ESM) is available at https://esm-db.eu/#/home, the webpage of the European Integrated Data Archive (EIDA) is available at http://www.orfeus-eu.org/data/eida/, and the webpage of the Incorporated Research Institutions for Seismology (IRIS) is available at https://www.iris.edu/hq. The REXELweb and WEBprocessing applications are available at https://esm-db.eu/#/rexel and https://esm-db.eu/processing/select, respectively.

The HDF Group, 1997–2015, ‘Hierarchical Data Format, version 5’, is available at https://www.hdfgroup.org/HDF5/. The documentation of the ar_pick algorithm in Obspy is available at https://docs.obspy.org/packages/autogen/obspy.signal.trigger.ar_pick.html, whereas the documentation of the recursive STA/LTA trigger algorithm in Obspy is available at https://docs.obspy.org/packages/autogen/obspy.signal.trigger.recursive_sta_lta_py.html .

This electronic supplement of this article contains: (1) Appendix S1 - describes the procedure to compute SNR_T; (2) Appendix S2 - describes the procedure for the automatic waveform trimming; (3) Appendix S3 - describes the method adopted to automatically set the cut-off frequencies of the bandpass filter; (4) Figures - supporting figures for the manuscript; (5) Table - testing dataset for the automatic recognition of more events on the same trace.

All websites were last accessed in October 2022.

Declaration of Competing Interests

The authors acknowledge there are no conflicts of interest recorded.

Acknowledgment

This study was funded by the ORFEUS project (ORFEUS Software Development Grant 2022) and by the Joint Research Unit of EPOS Italia (OS1: support to EPOS service providers - Engineering Strong Motion database, ESM - Access to Waveforms and products).

This study has also benefited from funding provided by the Italian Department of Civil Protection (DPC) in the framework of the Agreement A DPC - INGV 2020-2021 (WP7.2 Instrumental seismological databases). This paper does not necessarily represent DPC official opinion and policies.

The authors are grateful to the anonymous reviewers for their thorough revision and for their precious suggestions that brought significant improvements to the study.

References

Ancheta, T.D., R.B. Darragh, J.P. Stewart, E. Seyhan, W.J. Silva, B.S.J. Chiou, K.E. Wooddell, R.W. Graves, A.R. Kottke, D.M. Boore, and T. Kishida (2014). NGA-West2 database. Earthq Spectra 30 (3): 989–1005.

Akazawa, T. (2004). A technique for automatic detection of onset time of P-and S-Phases in strong motion records, 13th World Conference on Earthquake Engineering.

Akkar, S., and D. M. Boore (2009). On baseline corrections and uncertainty in response spectra for baseline variations commonly encountered in digital accelerograph records, Bull. Seismol. Soc.Am. 99, no. 3, 1671–1690.

Akkar, S., Z. Çağnan, E. Yenier, Ö. Erdoğan, M. A. Sandıkkaya, and P. Gülkan (2010). The recently compiled Turkish strong-motion database: Preliminary investigation for seismological parameters, J. Seismol. 14, no. 3, 457–479.

Arias, A. (1970). A measure of earthquake intensity, in Seismic Design of Nuclear Power Plants, R. Hansen (Editor), MIT press, Cambridge, Massachusetts.

Aur, K. A., J. Bobeck, A. Alberti, and P. Kay (2021). Pycheron: A Python- Based Seismic Waveform Data Quality Control Software Package. Seismological Research Letters; 92 (5): 3165–3178. doi: https://doi.org/10.1785/0220200418

Bahrampouri, M., A. Rodriguez-Marek, S. Shahi, and H. Dawood (2021). An updated database for ground motion parameters for KiK-net records, Earthq. Spectra 37, no. 1, doi: 10.1177/8755293020952447.

Bellagamba, X., R. Lee, and B. A. Bradley (2019). A neural network for automated quality screening of ground motion records from small magnitude earthquakes. Earthquake Spectra, 35(4), 1637-1661.

Bindi, D., S.-R. Kotha, G. Weatherill, G. Lanzano, L. Luzi, and F. Cotton (2018). The pan-European engineering strong motion (ESM), flatfile: Consistency check via residual analysis, Bull. Earthq. Eng. 17, no. 2, 583–602.

Boore, D. M. (2005). On pads and filters: Processing strong-motion data, Bull. Seismol. Soc. Am. 95, no. 2, 745–750.

Boore, D. M., A. Azari Sisi, and S. Akkar (2012). Using pad-stripped acausally filtered strong-motion data, Bull. Seismol. Soc. Am. 102, no. 2, 751–760.

Boore, D. M., and J. J. Bommer (2005). Processing of strong motion accelerograms: needs, options and consequences, Soil Dynam. Earthq. Eng. 25, no. 2, 93–115, doi: 10.1016/j.soildyn.2004.10.007.

Cara, F., G. Cultrera, G. Riccio, S. Amoroso, P. Bordoni, A. Bucci, E. D’Alema, M. D’Amico, L. Cantore, S. Carannante, R. Cogliano, G. Di Giulio, D. Di Naccio, D. Famiani, C. Felicetta, A. Fodarella, G. Franceschina, G. Lanzano, S. Lovati, L. Luzi, C. Mascandola, M. Massa, A.

Mercuri, G. Milana, F. Pacor, D. Piccarreda, M. Pischiutta, S. Pucillo, R. Puglia, M. Vassallo, G. Boniolo, G. Caielli, A. Corsi, R. de Franco, A. Tento, G. Bongiovanni, S. Hailemikael, G. Martini, A. Paciello, A. Peloso, F. Poggi, V. Verrubbi, M. R. Gallipoli, T. A. Stabile, and M. Mancini (2019). Temporary dense seismic network during the 2016 Central Italy seismic emergency for microzonation studies, Sci. Data 6, 182, doi: 10.1038/s41597-019-0188-1.

Casey, R., M. E. Templeton, G. Sharer, L. Keyson, B. R. Weertman, and T. Ahern (2018). Assuring the quality of IRIS data with MUSTANG, Seismol. Res. Lett. 89, no. 2A, 630–639.

Cauzzi, C., R. Sleeman, J. Clinton, J. D. Ballesta, O. Galanis, and P. Kastli (2016). Introducing the European raw strong motion database, Seismol. Res. Lett. 87, no. 4, 977–986.

Douglas, J and D.M. Boore (2011). High-frequency filtering of strong-motion records. Bull Earthq Eng 9 (2): 395–409.

D’Amico, M., C. Felicetta, E. Schiappapietra, F. Pacor, F. Galloviˇc, R. Paolucci, R. Puglia, G. Lanzano, S. Sgobba, and L. Luzi (2018). Fling Effects from Near-Source Strong-Motion Records: Insights from the 2016 Mw 6.5 Norcia, Central Italy, Earthquake. Seism. Res. Lett. 2018, 90, 659–671.

Haslinger, F., R. Basili, R. Bossu, C. Cauzzi, F. Cotton, H. Crowley, S. Custodio, L. Danciu, M. Locati, A. Michelini, I. Molinari, L. Ottemöller, and S. Parolai (2022). Coordinated and Interoperable Seismological Data and Product Services in Europe: the EPOS Thematic Core Service for Seismology. Annals of Geophysics, 65(2), DM213-DM213.

Hearne, M., E. M. Thompson, H. Schovanec, J. Rekoske, B. T. Aagaard, and C. B. Worden (2019). USGS automated ground motion processing software, USGS Software Release, doi: 10.5066/P9ANQXN3.

Hosseini, K., and K. Sigloch (2017). ObspyDMT: A python toolbox for retrieving and processing large seismological data sets, Solid Earth 8, 1047–1070.

Jones, J., E. Kalkan, C. Stephens, and P. Ng (2017). PRISM software processing and review interface for strong-motion data, Seismol. Res. Lett. 88, no. 3, 851–866.

Kalkan, E., and C. Stephens (2017). Systematic comparisons between PRISM version 1.0.0, BAP, and CSMIP ground-motion processing, U.S. Geol. Surv. Open-File Rept. 2017-1020, 108 pp., doi: 10.3133/ofr20171020.

Kleckner, J. K., K. B. Withers, E. M. Thompson, J. M. Rekoske, E. Wolin, and M. P. Moschetti (2021). Automated Detection of Clipping in Broadband Earthquake Records, Seismol. Res. Lett. 93, 880–896, doi: 10.1785/0220210028.

Krischer, L., J. Smith, W. Lei, M. Lefebvre, Y. Ruan, E. Sales de Andrade, N. Podhorszki, E. Bozdağ, and J. Tromp (2016). An Adaptable Seismic Data Format, Geophysical Journal International, Volume 207(2), 1003–1011, https://doi.org/10.1093/gji/ggw319.

Krischer, L., T. Megies, R. Barsch, M. Beyreuther, T. Lecocq, C. Caudron, and J. Wassermann (2015). ObsPy: A bridge for seismology into the scientific Python ecosystem. Computational Science & Discovery, 8(1), 014003.

Lanzano, G., L. Luzi, C. Cauzzi, J. Bienkowski, D. Bindi, J. Clinton, M. Cocco, M. D'Amico, J. Douglas, L. Faenza, C. Felicetta, F. Gallovic, D. Giardini, O.J. Ktenidou, V. Lauciani, M. Manakou, A. Marmureanu, E. Maufroy, A. Michelini, H. Özener, R. Puglia, R. Rupakhety, E. Russo, M. Shahvar, R. Sleeman, and N. Theodoulidis (2021). Accessing European Strong-Motion Data: An Update on ORFEUS Coordinated Services. Seismological Research Letters; 92 (3): 1642–1658. doi: https://doi.org/10.1785/0220200398

Lanzano, G., S. Sgobba, L. Luzi, R. Puglia, F. Pacor, C. Felicetta, M. D'Amico, F. Cotton, D. Bindi (2019). The pan-European engineering strong motion (ESM) flatfile: Compilation criteria and data statistics, Bull. Earthq. Eng. 17, 561–582.

Luzi, L., F. Pacor, R. Puglia, G. Lanzano, C. Felicetta, M. D'Amico, A. Michelini, L.Faenza, V. Lauciani, I. Iervolino, G. Baltzopoulos, and E. Chioccarelli (2017). The central Italy seismic sequence between August and December 2016: Analysis of strong- motion observations. Seismological Research Letters, 88(5), 1219-1231.

Luzi, L., R. Puglia, E. Russo, M. D'Amico, C. Felicetta, F. Pacor, G. Lanzano, U. Çeken, J. Clinton, G. Costa, L. Duni, E. Farzanegan, P. Gueguen, C. Ionescu, I. Kalogeras, H. Özener, D. Pesaresi, R. Sleeman, A. Strollo, and M. Zare (2016). The European strong-motion database: A platform to access accelerometric data, Seismol. Res. Lett. 87, no. 4, doi: 10.1785/0220150278.

Massa, M., D. Scafidi, C. Mascandola, and A. Lorenzetti (2022). Introducing ISMDq—A Web Portal for Real- Time Quality Monitoring of Italian Strong- Motion Data. Seismological Society of America, 93(1), 241-256.

Massa, M., E. D'Alema, C. Mascandola, S. Lovati, D. Scafidi, G. Franceschina, A. Gomez, S. Carannante, D. Piccarreda, M. Santi, and P. Augliera (2016). ISMD 2.0: the INGV real time strong-motion data sharing in the 2016 Amatrice (central Italy) seismic sequence, Ann. Geophys. 59, FAST TRACK 5, 2016, doi: 10.4401/AG-7193.

Massa, M., F. Pacor, L. Luzi, D. Bindi, G. Milana, F. Sabetta, A. Gorini, and S. Marcucci (2010). The ITalian ACcelerometric Archive (ITACA): Processing of strong-motion data, Bull. Earthq. Eng. 8, 1175–1187.

Massa, M., S. Lovati, G. Franceschina, E. D'Alema, S. Marzorati, S. Mazza, M. Cattaneo, G. Selvaggi, A. Amato, A. Michelini, and P. Augliera (2014). ISMD, a web portal for real time processing and dissemination of INGV Strong Motion Data, Seismol. Res. Lett. 85, no. 4, 863–877.

Pacor, F., Felicetta, C., Lanzano, G., Sgobba, S., Puglia, R., D'Amico, M., Russo, E., Baltzopoulos, G., and I. Iervolino (2018). NESS1: A Worldwide Collection of Strong- Motion Data to Investigate Near- Source Effects. Seismological Research Letters, 89(6), 2299–2313. https://doi.org/10.1785/0220180149

Pacor, F., R. Paolucci, G. Ameri, M. Massa, and R. Puglia (2011). Italian strong motion records in ITACA: Overview and record processing, Bull. Earthq. Eng. 9, no. 6, 1741–1759.

Pacor, F., R. Paolucci, L. Luzi, F. Sabetta, A. Spinelli, A. Gorini, M. Nicoletti, S. Marcucci, L. Filippi, and M. Dolce (2011). Overview of the Italian strong motion database ITACA 1.0, Bull. Earthq. Eng. 9, no. 6, 1723–1739.

Paolucci, R., F. Pacor, R. Puglia, G. Ameri, C. Cauzzi, and M. Massa (2011). Record processing in ITACA, the new Italian strong motion database, in Earthquake Data in Engineering Seismology Predictive Models, Data Management and Networks, S. Akkar, P. Gülkan, and T. van Eck (Editors), Springer, Dordrecht, The Netherlands, 99–113, ISBN: 978-94- 007-0151-9 (printed version) 978-94-007-0152-6 (e-book version).

Papazafeiropoulos, G., and V. Plevris (2018). OpenSeismoMatlab: A new open-source software for strong ground data processing, Heliyon 4, doi: 10.1016/j.heliyon.2018.e00784.

Petersen, G. M., S. Cesca, M. Kriegerowski, and AlpArray Working Group. (2019). Automated quality control for large seismic networks: Implementation and application to the AlpArray seismic network. Seismological Research Letters, 90(3), 1177-1190.

Puglia, R., E. Russo, L. Luzi, M. D’Amico, C. Felicetta, F. Pacor, and G. Lanzano (2018). Strong motion processing service: A tool to access and analyze earthquakes strong motion waveforms, Bull. Earthq. Eng. 16, 2641–2651.

Rekoske, J. M., E. M. Thompson, M. P. Moschetti, M. G. Hearne, B. T. Aagaard, and G. A. Parker (2020). The 2019 Ridgecrest, California, earthquake sequence ground motions: Processed records and derived intensity metrics, Seismol. Res. Lett. 91, 2010–2023.

Ringler, A. T., M. T. Hagerty, J. Holland, A. Gonzales, L. S. Gee, J. D. Edwards, D. Wilson, and A. M. Baker (2015). The data quality analyzer: A quality control program for seismic data, Comput. Geosci. 76, 96–111.

Schiappapietra, E., C. Felicetta, and M. D'Amico (2021). Fling-Step Recovering from Near-Source Waveforms Database. Geosciences, 11, 67., https://doi.org/10.3390/geosciences11020067.

Sgobba, S., C. Felicetta, G. Lanzano, F. Ramadan, M. D'Amico, and F. Pacor (2021). NESS2.0: An updated version of the worldwide dataset for calibrating and adjusting ground‐ motion models in near source. Bulletin of the Seismological Society of America, 111(5), 2358-2378.

Sharer, G., J. Callahan, and R. Casey (2017). iris‐ edu/ispaq, Github, available at https://github.com/iris-edu/ispaq (last accessed March 2021)

Trnkoczy, A., P. Bormann, W. Hanka, L.G. Holcomb, and R.L., Nigbor (2012). Site selection, preparation and installation of seismic stations. In New Manual of Seismological Observatory Practice 2 (NMSOP-2) (pp. 1-139). Deutsches GeoForschungsZentrum GFZ.

Weber, B., J. Becker, W. Hanka, A. Heinloo, M. Hoffmann, T. Kraft, D. Pahlke, J. Reinhardt, J. Saul, and H. Thoms (2007). SeisComP3 automatic and interactive real time data processing, Geophys. Res. Abstr. 9, 09219.

Zaccarelli, R., D. Bindi, A. Strollo, J. Quinteros, and F. Cotton (2019). Stream2segment: An open-source tool for downloading, processing, and visualizing massive event-based seismic waveform datasets, Seismol. Res. Lett. 90, no. 5, 2028–2038.

Zaccarelli, R., D. Bindi, and A. Strollo (2021). Anomaly detection in seismic data–metadata using simple machine- learning models. Seismological Society of America, 92(4), 2627-2639.

Claudia Mascandola
Maria D'Amico
Emiliano Russo
Lucia Luzi
Istituto Nazionale di Geofisica e Vulcanologia (INGV)
Via Alfonso Corti 12
20133 Milano, Italy
claudia.mascandola@ingv.it
maria.damico@ingv.it
emiliano.russo@ingv.it
lucia.luzi@ingv.it

List of Figure Captions

Figure 1: Geographic distribution of a) events and b) stations included in ESM. A zoom for the EuroMediterranean region is reported for both panels, along with a pie chart showing the statistics by country.

Figure 2: a) Magnitude-Distance distribution of all the ESM waveforms, with b) the number of waveforms per year related to the last 20 years. The good or bad quality flag was assigned after manual revision (ESM database, see Data and Resources).

Figure 3: workflow for data processing in ESMpro. Dashed arrows: metadata flow; solid arrows: data flow. The processing methods are PAO11 (Paolucci et al., 2011) and eBASCO (Schiappapietra et al., 2011). CV: uncorrected waveforms; AP: automatically processed with PAO11; MP: manually processed with PAO11. AB: automatically processed with eBASCO; MB: manually processed with eBASCO.

Figure 4: Features identified by the quality check implemented in ESMpro. The vertical green and red lines indicate the P- and S- wave arrivals, respectively. Solid lines: automatic picking; dashed lines: theoretical arrivals. The green and red boxes indicate respectively the 4s noise and signal windows, adopted for the SNR_T computation. Example of records that cannot be automatically a) trimmed or b) picked. c) Good quality data; and d) Low quality data. Records with e) SNR_T > 60 dB; f) PGA > 2 g; g) unrealistic horizontal component; h) unreliable P-wave arrival; i) multiple events; and j) restricted frequency passband.

Figure 5: Distribution of SNR_T values on the ESM data. The black line indicates the mean value and the grey shadow the 68% confidence interval. The red dashed line and the red circle mark the threshold of 6 dB and the anomalous SNR_T distribution, respectively.

Figure 6: decision matrix in ESMpro.

Figure 7: Automatic setting of the cut-off frequencies for the bandpass filter. As an example, the records of the event EMSC-20150808_0000064 at the IT.TOR station are reported. a) Accelerometric time series. The red dashed line marks the automatic P-wave arrival; the blue and red boxes indicate the noise and signal windows respectively. b) FFT of signal (blue curves) and noise (red curves). c) Signal-to-noise ratio in the frequency domain (SNR_F). The selected SNR threshold is indicated by a dashed red line and the cut-off frequencies of the bandpass filter are given by the vertical grey lines.

Figure 8: Comparison between ESMpro outcomes and metadata of the ESM manually processed waveforms. Quality check on the ESM good quality (a) and bad quality (b) data. Automatic setting for startime (b) and endtime (c), along with lc (e) and hc (f) frequencies. The automatic settings for the records with more events detected are highlighted in red.

Figure 1

Click here to access/download;Figure;Fig1.jpg

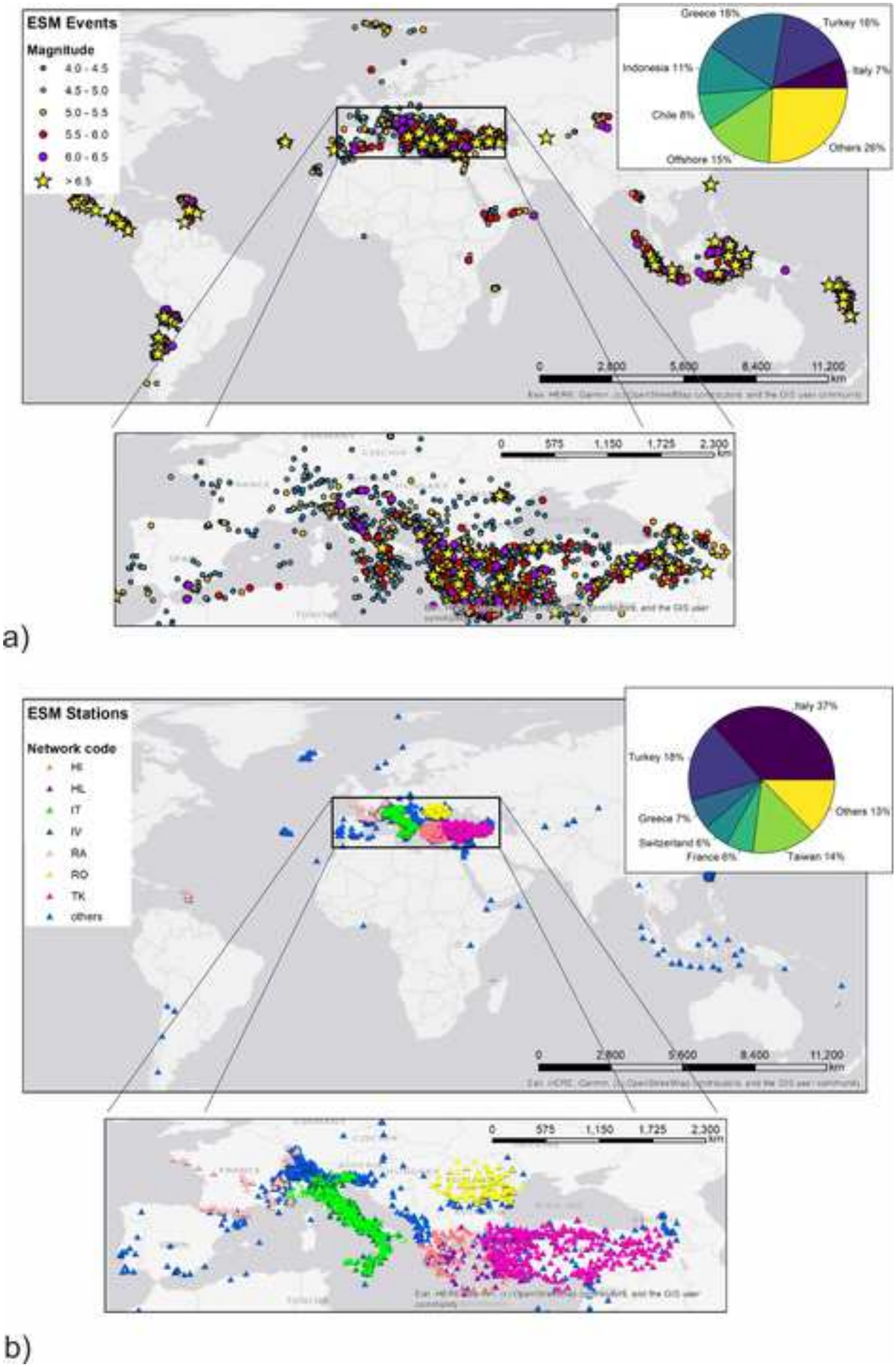

Figure 2

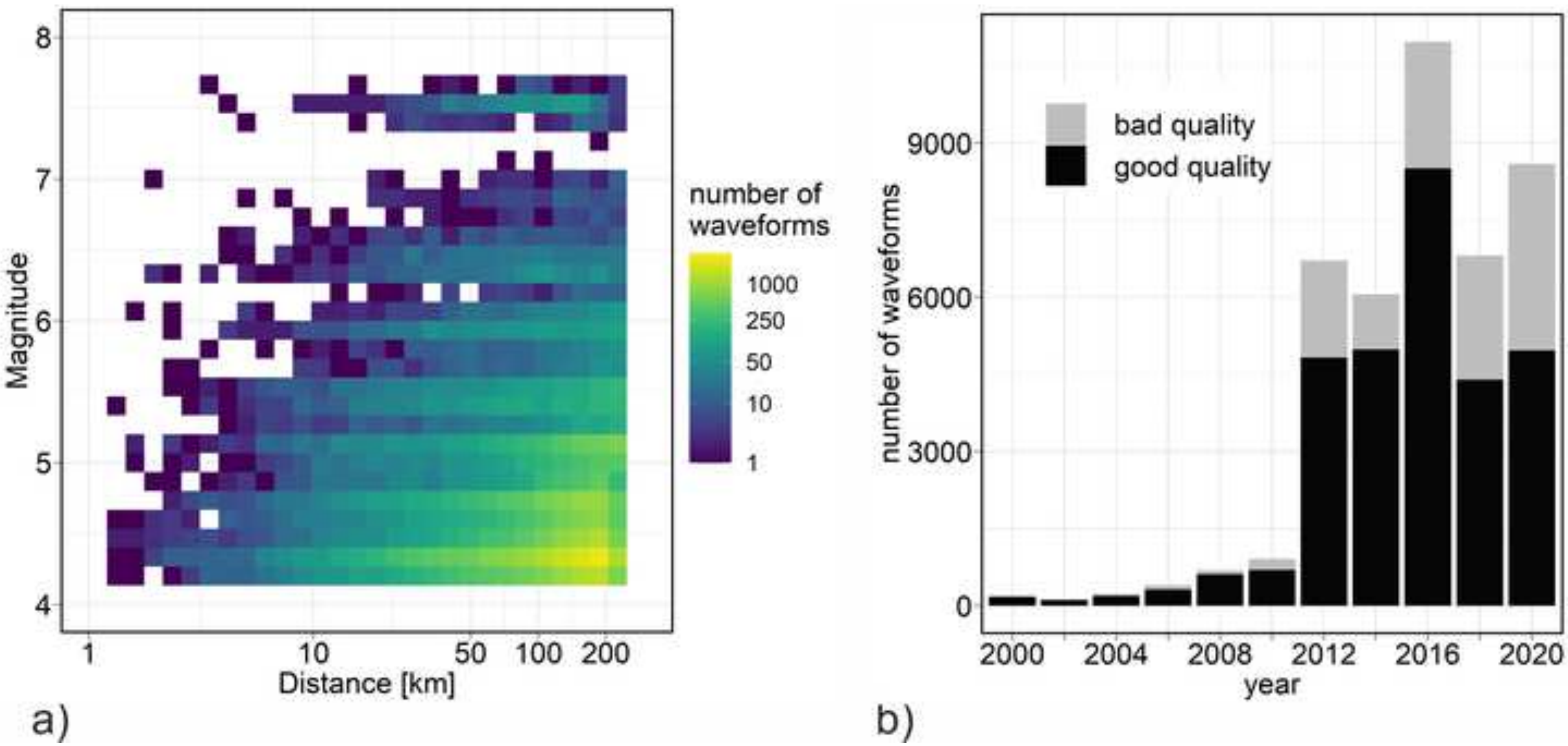

Magnitude
8
7
6
5
4
1
10
50
100
200
Distance [km]
number of waveforms
1000
250
50
10
1
a)
bad quality
good quality
number of waveforms
9000
6000
3000
0
2000
2004
2008
2012
2016
2020
year
b)

Figure 3

Click here to access/download;Figure;Fig3.jpg

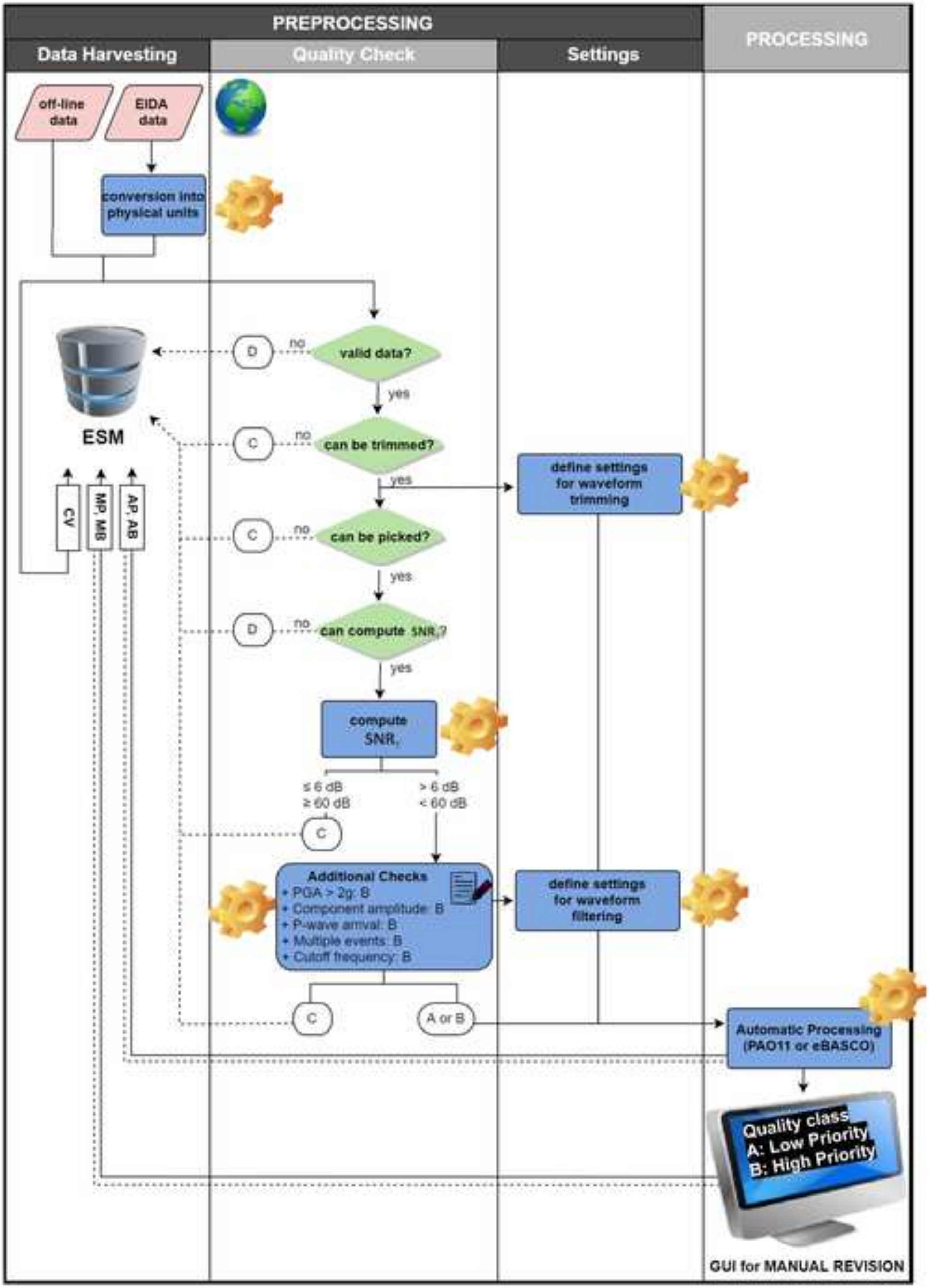

Figure 4

Click here to access/download;Figure;Fig4.jpg

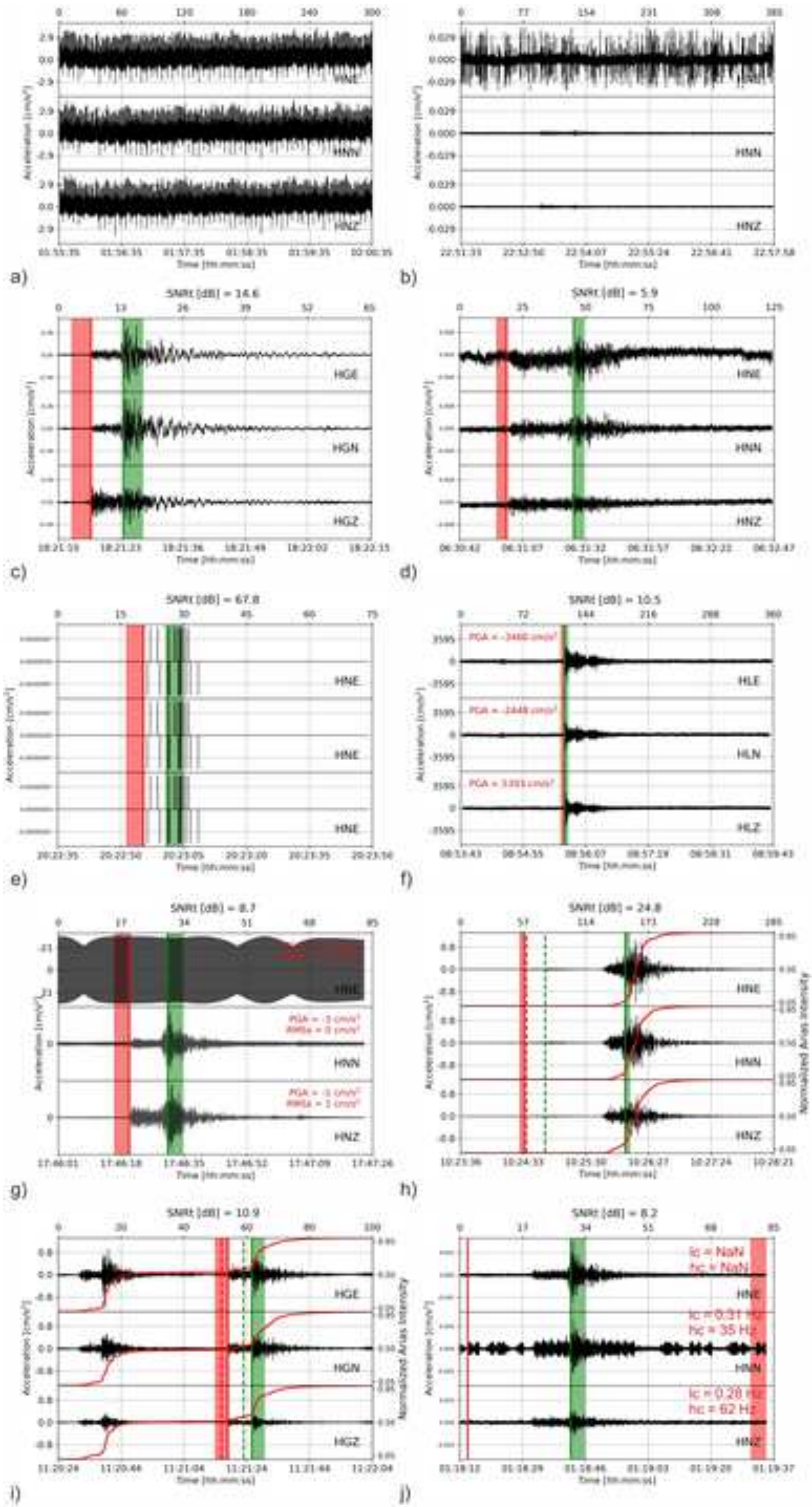

Figure 5

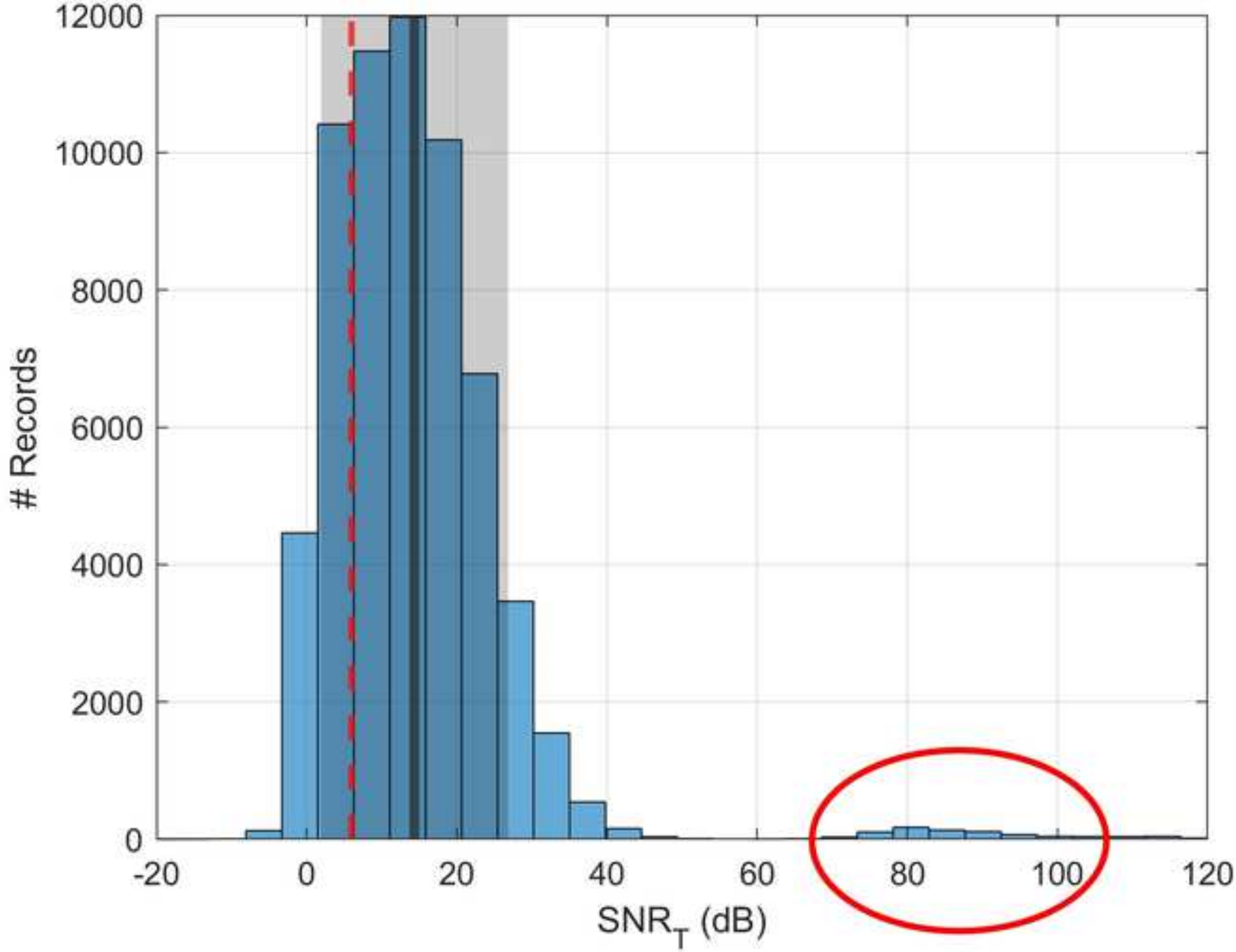

12000
10000
8000
6000
4000
2000
0
Records
-20
0
20
40
60
80
100
120
SNR_T (dB)

Figure 6

Click here to access/download;Figure;Fig6.jpg

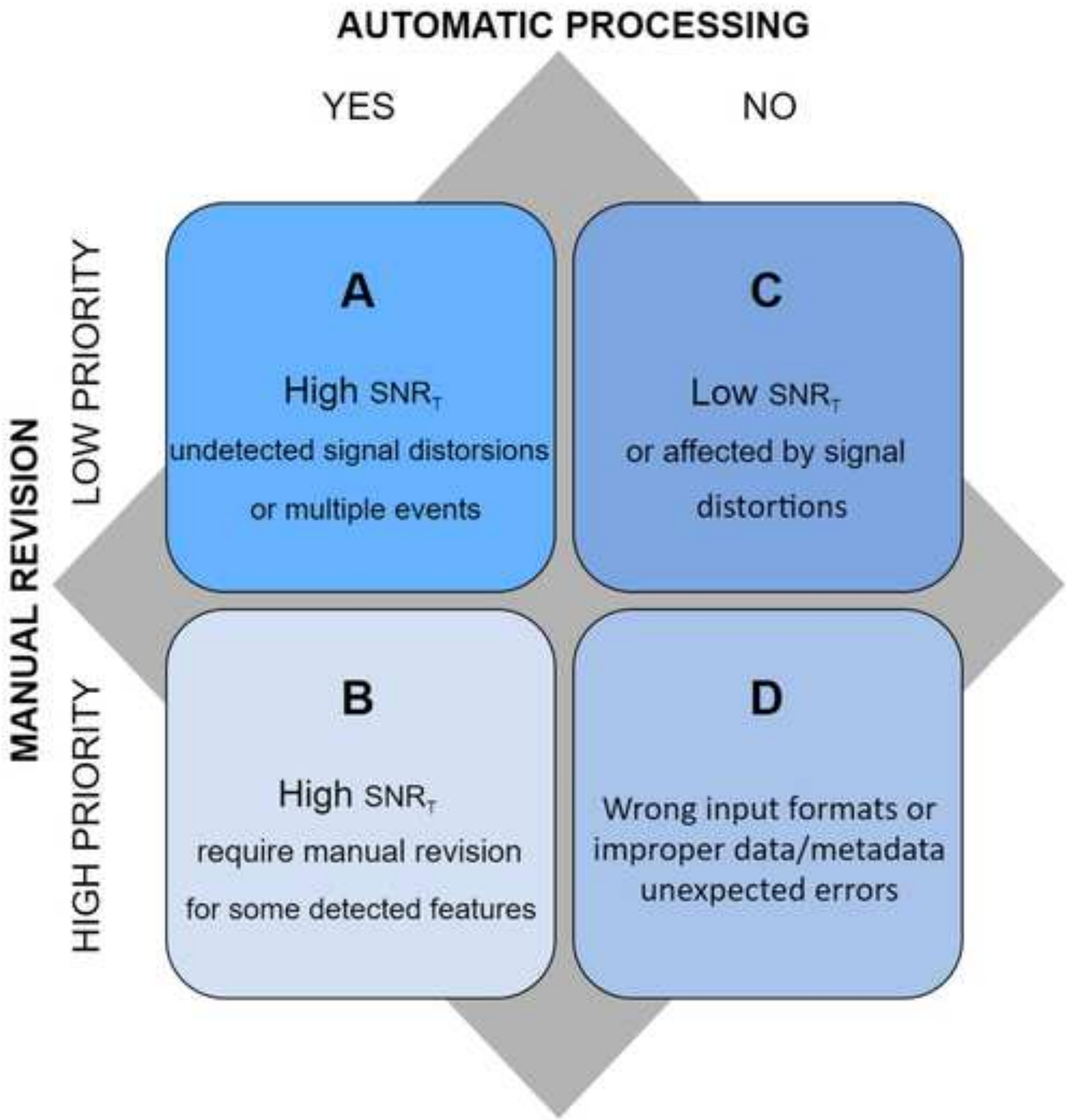

Figure 7

Click here to access/download;Figure;Fig7.jpg

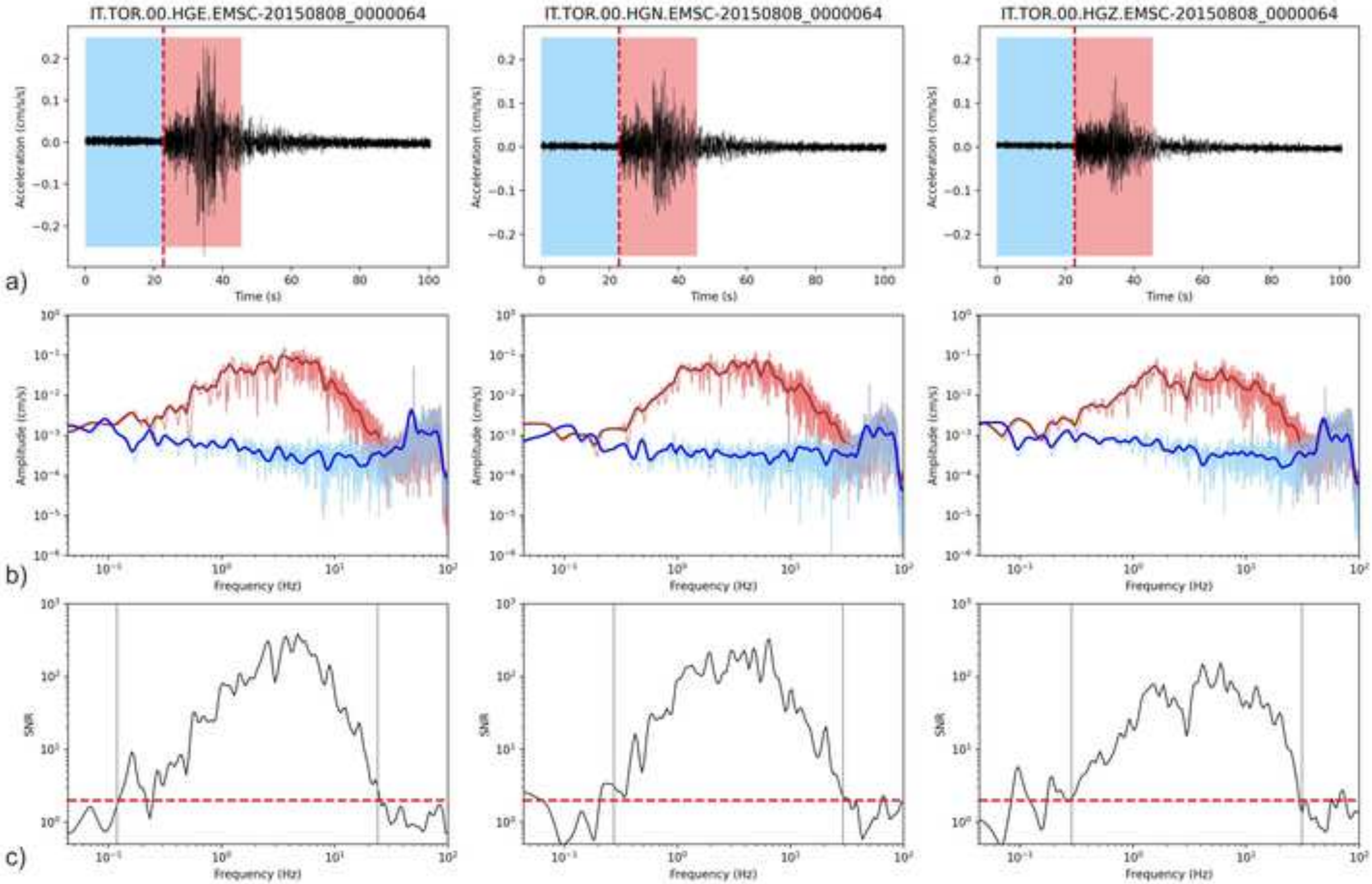

Figure 8 Click here to access/download;Figure;Fig8.jpg

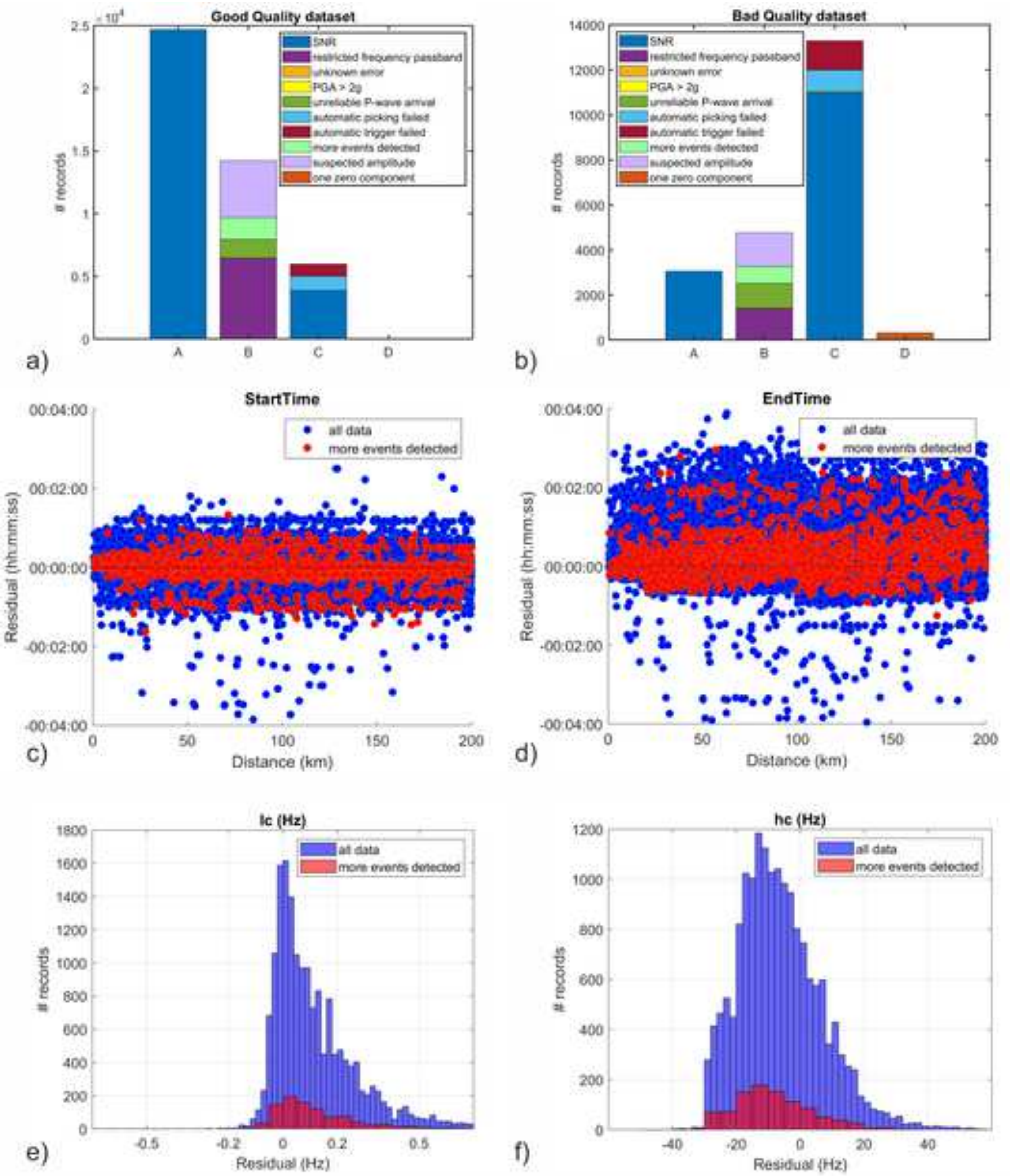

Tables

Table 1: Additional checks considered for the quality class assignment after SNR_T computation. lc and hc are the low-cut and high-cut frequency, respectively, of the Butterworth bandpass filter. PGA: Peak Ground Acceleration; PGD: Peak Ground Displacement; RMS: Root Mean Square (quadratic mean).

#	**Warnings**	**Quality Class**	**Issues**
1	Extreme PGA	B	The PGA is greater than 2*g* on at least one of the three components.
2	Suspected amplitude	B	One horizontal component is more than twice the other or the vertical component is more than 3 times the horizontals (on PGA or RMS). Data should be manually revised.
3	Unreliable P-wave arrival	B	If the lag between the theoretical P-wave arrival and the 5% of the Normalized Arias Intensity is greater than 20s, the waveform may not be trimmed properly (see Appendix S2).
4	Multiple events	B	More events are detected on the same trace, suggested manual revision.
5	Restricted frequency passband	B	If lc > 0.4 Hz The low-cut frequency of the bandpass filter is too high; try to extend the bandwidth by manual revision. If hc < 20 Hz The high-cut frequency of the bandpass filter is too low; try to extend the bandwidth by manual revision.

Electronic Supplement to

ESMpro: a proposal for improved data management for the Engineering Strong Motion database (ESM)

by Claudia Mascandola, Maria D'Amico, Emiliano Russo and Lucia Luzi

This electronic supplement contains:

- Appendix S1 - describes the procedure to compute SNR_T;
- Appendix S2 - describes the procedure for the automatic waveform trimming;
- Appendix S3 - describes the method adopted to automatically set the cut-off frequencies of the bandpass filter;
- Figures - supporting figures for the manuscript;
- Table - testing dataset for the automatic recognition of more events on the same trace.

Appendix S1

The procedure to compute SNR_T is the following:

- 2^{nd} order acausal Butterworth bandpass filter between 2-8 Hz to allow a better application of the picking algorithm;
- picking of P- and S- waves with the ar_pick algorithm in Obspy (see Data and Resources), which includes a combination of AR-AIC and STA/LTA algorithms (Akazawa, 2004);
- computation of the Root Mean Square (RMS_S) on a strong-motion time window of 4 s, starting from the S- wave picking;
- computation of the Root Mean Square (RMS_N) on a pre-event noise window of 4 s, before P-wave picking. If the length of the pre-event noise window is shorter, it takes 4s from the end of the trace;

- computation of SNR_T as the ratio between RMS_S and RMS_N, for each ground-motion component;
- computation of the mean SNR_T for the three-component seismic records.

Appendix S2

The raw data downloaded from continuous streams (considering the event metadata) are often featured by long noise windows before or after the event, which may be annoying for engineering and practitioners that adopt these waveforms in several applications. To this aim, we adopt the following procedure to refine the waveform trimming around the target event:

- 2^{nd} order acausal Butterworth bandpass filter between 2 -8 Hz to allow a better application of the trigger algorithm;
- the recursive short-time average/long-time average (STA/LTA) algorithm in Obspy (see Data and Resources) is applied with STA = 1s and LTA = 8s;
- Trigger On (T1) at the STA/LTA threshold of 2.5;
- Trigger Off (T2) at the STA/LTA threshold of 0.3;
- selection of the trigger closer to the theoretical P wave arrival: the theoretical P wave arrival is adopted to discard false triggers and select the correct trigger in case of multiple events;
- first sample: T1 - 20s. If the 3-component waveform does not have enough pre-event seconds, a zero-padding is applied;
- last Sample: T2 + dt, where dt is a time interval, which depends on the source-to-site distance (D) based on empirical observations (see table below).

dt [s]	Condition on D [km]
20	D < 20
40	20 < D < 100

60	100 < D < 200
80	D > 200

Appendix S3

For the SNR_F computation we consider the entire traces uploaded on ESM, before waveform trimming, in order to preserve all available pre-event noise. The method adopted to automatically set the cut-off frequencies of the bandpass filter is described by the following steps:

- selection of the noise window before the P wave arrival (all available pre-event noise);
- selection of the signal window after the P wave arrival. The noise and signal windows have the same length, constrained by the available pre-event noise;
- computation of the Fast Fourier Transform on the signal (FFT_S) and noise (FFT_N) windows;
- resampling of the FFT and application of a Konno-Ohmachi smoothing (b=40);
- computation of the of the Signal-to-Noise Ratio in the frequency domain, SNR_F, as the ratio of (FFT_S - FFT_N) and FFT_N for each ground motion component;
- the SNR_F threshold of 2 is adopted to select the low-cut frequency (lc) and the high-cut frequency (hc);
- selection of lc: we start from the central peak of the SNR_F curve and we move leftwards with a mobile window where the average SNR_F is computed. The mobile window is centered on lc and ranges from lc/$\sqrt{2}$ to lc·$\sqrt{2}$. The lc frequency is selected when the SNR_F, computed in the mobile window, is lower than 2. The minimum value of lc is the inverse of the time-length of the pre-event noise window;
- selection of hc*:* same method adopted for lc, but moving rightwards with a mobile window that ranges from hc/$\sqrt{1.3}$ to hc·$\sqrt{1.3}$. The maximum value of hc is the Nyquist frequency (f_N).

- If the SNR_F curve is always above the predefined threshold of 2, the lc frequency depends on magnitude ranges (Puglia et al., 2018). On the contrary, the hc frequency is set at 40 Hz to avoid anthropic and instrumental noise often observed at higher frequencies (Trnkoczy et al., 2012).

Figures

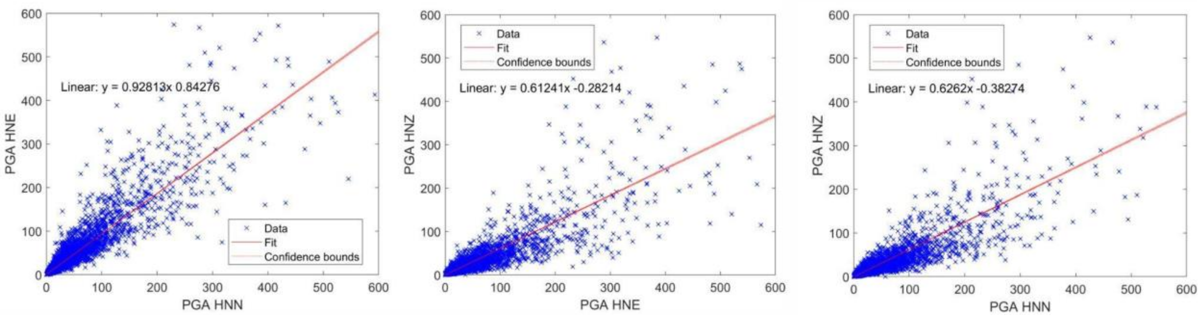

Figure S1: PGA distribution on the ESM data. Left: relation between PGA of horizontal components (HNN, HNE). Central: relation between East and vertical components. Right: relation between North and vertical components. The horizontal components have an average PGA ratio of 0.9 and they are about 1.6 times the vertical one.

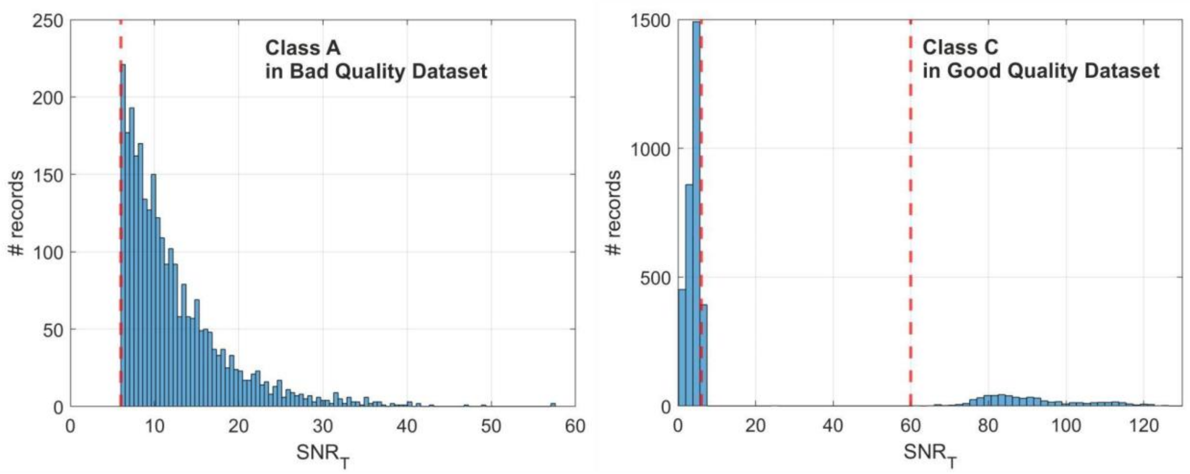

Figure S2: Distribution of SNR_T values on the records of the bad quality dataset classified in A (left) and those of the good quality dataset classified in C (right). The SNR_T thresholds of 6 dB and 60 dB are marked by a vertical dashed line.

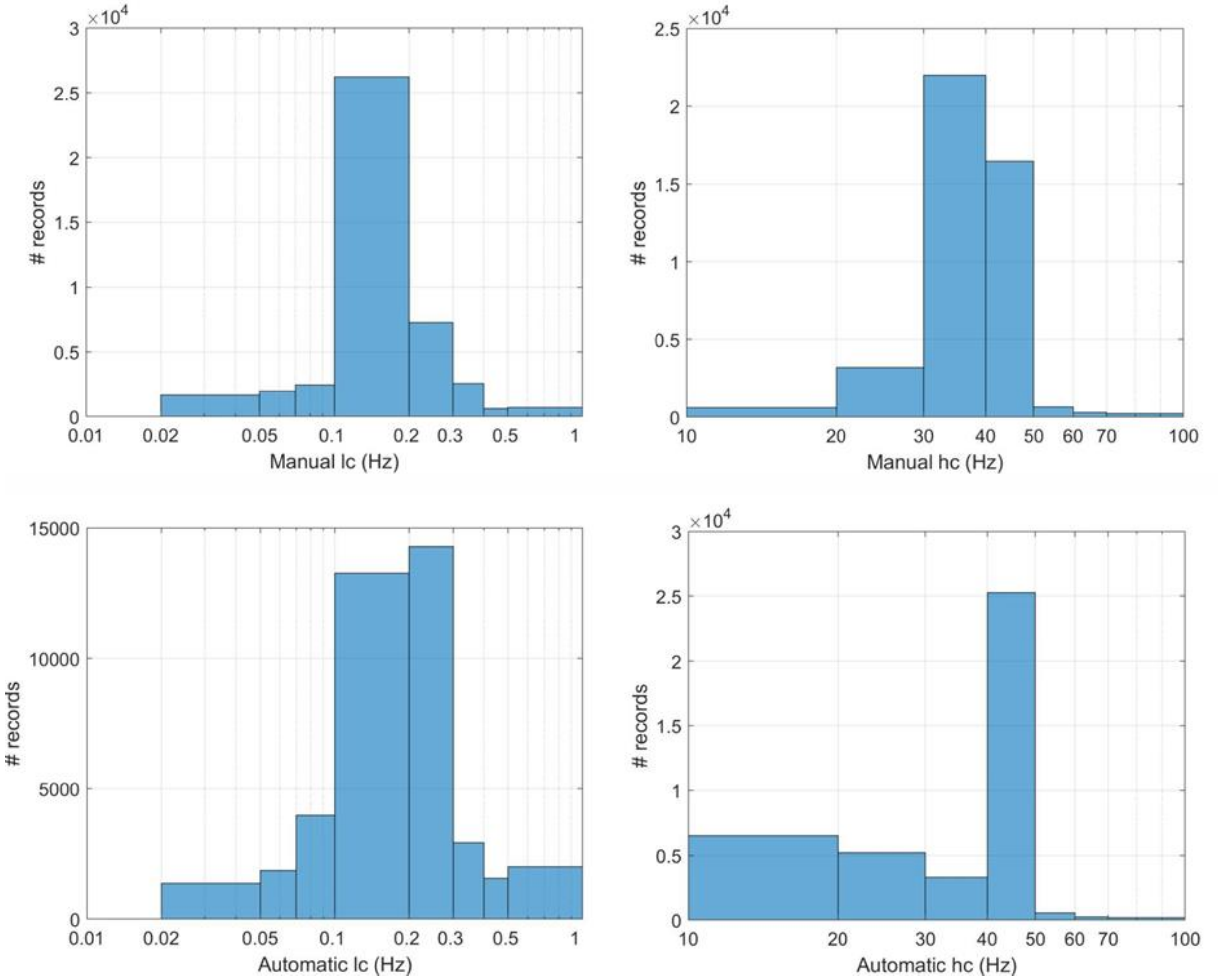

Figure S3: Distribution of manual lc and hc frequencies (top panels), besides automatic lc e hc frequencies (bottom panels) on ESM public data.

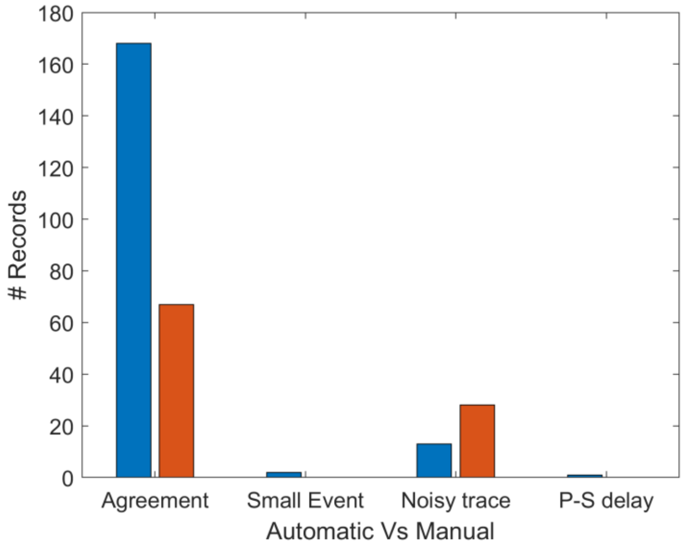

Figure S4: Testing the automatic recognition of multiple events. The testing dataset is composed of 184 good quality (blue) and 95 bad quality (red) records extracted from the ESM database. *Agreement*: the automatic and manual recognition are in agreement; *Small event*: a small event escaped the automatic recognition of multiple events; *Noisy trace*: erroneous automatic recognition of multiple events due to a noisy trace; *P-S delay*: erroneous automatic recognition of multiple events for the delay between P and S-wave arrivals.

Tables

Table S1: dataset adopted for testing the recognition of multiple events. MP man: visual inspection of multiple events; MP auto: automatic recognition of multiple events. 1: recognized multiple events; 0: unrecognized multiple events. ESM quality is good or bad if the record is flagged as good or bad quality on the ESM database, respectively.

#	filename	MP man	MP auto	note	ESM quality
1	CX.PB02..HL.EMSC-20170618_0000020.h5	0	0		good
2	CX.PATCX..HL.EMSC-20170618_0000020.h5	0	0		good
3	C.GO01..HN.EMSC-20170618_0000020.h5	0	0		good

4	CX.PB08..HL.EMSC-20170618_0000020.h5	0	0		good
5	CX.PB11..HL.EMSC-20170618_0000020.h5	0	0		good
6	CX.PB01..HL.EMSC-20170618_0000020.h5	0	0		good
7	IU.LVC.20.HN.EMSC-20160405_0000100.h5	0	0		good
8	G.SANVU.00.HN.EMSC-20130419_0000054.h5	0	0		good
9	PR.ROPR..HN.EMSC-20191027_0000076.h5	0	0		good
10	4A.MI02..HN.EMSC-20090407_0000144.h5	1	1		good
11	4A.MI03..HN.EMSC-20090407_0000144.h5	1	1		good
12	IV.RM08..HN.EMSC-20090407_0000144.h5	1	1		good
13	3H.NO13..HH.EMSC-20090407_0000144.h5	0	0		good
14	IV.RM04..HN.EMSC-20090407_0000144.h5	1	1		good
15	IV.RM08..HN.EMSC-20090407_0000144.h5	1	1		good
16	IV.RM14..HN.EMSC-20090407_0000144.h5	1	1		good
17	IV.BAG8..HN.EMSC-20120527_0000081.h5	0	0		good
18	IV.T0819..HN.EMSC-20120609_0000005.h5	1	1		good
19	IV.PIPA..HN.EMSC-20120704_0000050.h5	0	0		good
20	IV.T0701..HN.EMSC-20120828_0000070.h5	1	0	small event	good
21	IV.ACER..HN.EMSC-20121016_0000066.h5	0	0		good
22	IV.CELI..HN.EMSC-20121016_0000066.h5	0	0		good
23	IV.SALB..HN.EMSC-20121016_0000066.h5	0	0		good
24	IV.SERS..HN.EMSC-20121016_0000066.h5	0	0		good
25	MN.PDG..HL.EMSC-20121112_0000088.h5	1	1		good
26	IV.PIPA..HN.EMSC-20130324_0000133.h5	0	0		good
27	IV.CELI..HN.EMSC-20130815_0000084.h5	1	1		good
28	IV.JOPP..HN.EMSC-20130815_0000084.h5	1	1		good
29	IV.PLAC..HN.EMSC-20130815_0000084.h5	1	1		good
30	MN.CUC..HN.EMSC-20130815_0000084.h5	1	1		good
31	IV.PLAC..HN.EMSC-20130902_0000004.h5	1	0	P-S delay	good
32	IV.SERS..HN.EMSC-20130902_0000004.h5	0	0		good
33	IV.PP3..HN.EMSC-20140429_0000089.h5	1	1		good
34	BA.PZUN..HL.EMSC-20140604_0000074.h5	1	1		good
35	BA.PZUN..HL.EMSC-20140606_0000048.h5	1	1		good
36	IV.BSSO..HN.EMSC-20140606_0000048.h5	0	1	noisy	good
37	IV.CELI..HN.EMSC-20140606_0000048.h5	0	0		good

38	IV.MRLC..HN.EMSC-20140606_0000048.h5	0	0		good
39	IV.EPOZ..HN.EMSC-20140607_0000040.h5	0	1	noisy	good
40	IV.NDIM..HN.EMSC-20140828_0000047.h5	1	1		good
41	IV.SBPO..HN.EMSC-20140907_0000025.h5	1	1		good
42	IV.ATPC..HN.EMSC-20141003_0000008.h5	0	1	noisy	good
43	IV.BULG..HN.EMSC-20141009_0000056.h5	1	1		good
44	IV.IMOL..HN.EMSC-20141017_0000007.h5	1	1		good
45	IV.MURB..HN.EMSC-20141017_0000007.h5	0	1	noisy	good
46	IV.EUCT..HN.EMSC-20141206_0000048.h5	1	1		good
47	IV.FIR..HN.EMSC-20141219_0000002.h5	1	1		good
48	IV.FIR..HN.EMSC-20141219_0000035.h5	0	1	noisy	good
49	IV.FIAM..HN.EMSC-20141219_0000039.h5	0	0		good
50	IV.SFI..HN.EMSC-20141219_0000039.h5	0	1	noisy	good
51	IV.SACS..HN.EMSC-20141219_0000115.h5	0	0		good
52	IV.SFI..HN.EMSC-20141219_0000115.h5	1	1		good
53	IV.BDI..HN.EMSC-20141220_0000008.h5	1	1		good
54	IV.CAFI..HN.EMSC-20141220_0000008.h5	1	1		good
55	IV.CPGN..HN.EMSC-20141220_0000008.h5	1	1		good
56	IV.CRMI..HN.EMSC-20141220_0000008.h5	1	1		good
57	IV.MGAB..HN.EMSC-20141220_0000008.h5	1	1		good
58	IV.MTRZ..HN.EMSC-20141220_0000008.h5	1	1		good
59	IV.OSSC..HN.EMSC-20141220_0000008.h5	1	1		good
60	IV.SACS..HN.EMSC-20141220_0000008.h5	1	1		good
61	IV.SFI..HN.EMSC-20141220_0000008.h5	0	0		good
62	IV.ZCCA..HN.EMSC-20141220_0000008.h5	1	1		good
63	MN.VLC..HN.EMSC-20141220_0000008.h5	1	1		good
64	IV.FIR..HN.EMSC-20150123_0000041.h5	1	1		good
65	IV.TREG..HN.EMSC-20150123_0000041.h5	0	0		good
66	IV.BDI..HN.EMSC-20150123_0000096.h5	1	1		good
67	IV.CRMI..HN.EMSC-20150123_0000096.h5	1	1		good
68	IV.OSSC..HN.EMSC-20150303_0000086.h5	1	1		good
69	IV.JOPP..HN.EMSC-20150329_0000038.h5	1	1		good
70	MN.CEL..HN.EMSC-20150329_0000038.h5	1	1		good
71	IV.CELI..HN.EMSC-20150415_0000060.h5	0	0		good
72	IV.JOPP..HN.EMSC-20150415_0000060.h5	0	0		good

73	IV.MCEL..HN.EMSC-20150415_0000060.h5	0	0		good
74	IV.PLAC..HN.EMSC-20150415_0000060.h5	0	0		good
75	IV.SERS..HN.EMSC-20150415_0000060.h5	0	0		good
76	MN.TIP..HN.EMSC-20150415_0000060.h5	0	0		good
77	IV.MRB1..HN.EMSC-20150416_0000041.h5	1	1		good
78	IV.CRMI..HN.EMSC-20150424_0000065.h5	0	0		good
79	IV.SBPO..HN.EMSC-20150424_0000065.h5	1	1		good
80	ST.RONC..HN.EMSC-20150424_0000065.h5	1	1		good
81	IV.JOPP..HN.EMSC-20150509_0000023.h5	0	0		good
82	IV.MCEL..HN.EMSC-20150509_0000023.h5	0	0		good
83	IV.PLAC..HN.EMSC-20150509_0000023.h5	0	0		good
84	IV.SERS..HN.EMSC-20150509_0000023.h5	0	0		good
85	MN.CEL..HN.EMSC-20150509_0000023.h5	0	0		good
86	MN.TIP..HN.EMSC-20150509_0000023.h5	0	0		good
87	MN.AQU..HL.EMSC-20150529_0000093.h5	0	1	noisy	good
88	IV.SBPO..HN.EMSC-20150722_0000055.h5	1	1		good
89	IV.ATVO..HN.EMSC-20160824_0000010.h5	1	1		good
90	IV.CADA..HN.EMSC-20160824_0000010.h5	1	1		good
91	IV.FEMA..HN.EMSC-20160824_0000010.h5	1	1		good
92	IV.GUMA..HN.EMSC-20160824_0000010.h5	1	1		good
93	IV.INTR..HN.EMSC-20160824_0000010.h5	1	1		good
94	IV.PP3..HN.EMSC-20160824_0000010.h5	1	1		good
95	IV.SACS..HN.EMSC-20160824_0000010.h5	1	1		good
96	IV.FIAM..HN.EMSC-20160824_0000024.h5	1	1		good
97	IV.TERO..HN.EMSC-20160824_0000024.h5	1	1		good
98	IV.NRCA..HN.EMSC-20160824_0000036.h5	1	1		good
99	IV.FIAM..HN.EMSC-20160824_0000192.h5	1	0	small event	good
100	IV.MGAB..HN.EMSC-20160824_0000295.h5	1	1		good
101	IV.T1214..HN.EMSC-20160824_0000295.h5	1	1		good
102	IV.T1213..HN.EMSC-20160826_0000134.h5	1	1		good
103	IV.ATLO..HN.EMSC-20160827_0000015.h5	0	0		good
104	IV.ATTE..HN.EMSC-20160827_0000015.h5	0	0		good
105	IV.COR1..HN.EMSC-20160827_0000015.h5	0	1	noisy	good
106	IV.GUMA..HN.EMSC-20160827_0000015.h5	0	1	noisy	good
107	IV.RM33..HN.EMSC-20160828_0000017.h5	1	1		good

108	IV.T1243..HN.EMSC-20160828_0000017.h5	1	1		good
109	IV.T1299..HN.EMSC-20160831_0000063.h5	0	1	noisy	good
110	XO.CP01..HN.EMSC-20160831_0000063.h5	0	0		good
111	IV.T1213..HN.EMSC-20160831_0000092.h5	1	1		good
112	XO.CP06..HN.EMSC-20160831_0000101.h5	0	0		good
113	XO.MN09..HN.EMSC-20160831_0000101.h5	1	1		good
114	IV.MNTP..HN.EMSC-20160901_0000051.h5	1	1		good
115	IV.ATCC..HN.EMSC-20160915_0000064.h5	1	1		good
116	IV.ATFO..HN.EMSC-20160915_0000064.h5	1	1		good
117	IV.FEMA..HN.EMSC-20160915_0000064.h5	1	1		good
118	IV.RM33..HN.EMSC-20160915_0000064.h5	1	1		good
119	IV.SEF1..HN.EMSC-20160915_0000064.h5	1	1		good
120	IV.T1211..HN.EMSC-20160915_0000064.h5	1	1		good
121	IV.T1214..HN.EMSC-20160915_0000064.h5	1	1		good
122	IV.T1243..HN.EMSC-20160915_0000064.h5	1	1		good
123	IV.TRE1..HN.EMSC-20160915_0000064.h5	1	1		good
124	XO.CP06..HN.EMSC-20160915_0000064.h5	1	1		good
125	XO.CV01..HN.EMSC-20160915_0000064.h5	1	1		good
126	XO.CV02..HN.EMSC-20160915_0000064.h5	1	1		good
127	XO.CV03..HN.EMSC-20160915_0000064.h5	1	1		good
128	XO.MN06..HN.EMSC-20160915_0000064.h5	1	1		good
129	XO.MN08..HN.EMSC-20160915_0000064.h5	1	1		good
130	3A.MZ10..HN.EMSC-20161004_0000061.h5	1	1		good
131	IV.T1215..HN.EMSC-20161026_0000105.h5	1	1		good
132	IV.T1243..HN.EMSC-20161026_0000105.h5	0	0		good
133	IV.T1299..HN.EMSC-20161026_0000140.h5	0	1	noisy	good
134	IV.CAFI..HN.EMSC-20161026_0000171.h5	0	0		good
135	IV.SNTG..HN.EMSC-20161026_0000171.h5	0	1	noisy	good
136	IV.T1215..HN.EMSC-20161026_0000171.h5	1	1		good
137	IV.T1216..HN.EMSC-20161026_0000171.h5	1	1		good
138	IV.T1214..HN.EMSC-20161027_0000001.h5	1	1		good
139	IV.T1216..HN.EMSC-20161027_0000001.h5	1	1		good
140	IV.ATTE..HN.EMSC-20161027_0000008.h5	0	0		good
141	IV.CAFI..HN.EMSC-20161027_0000016.h5	0	0		good
142	IV.MMUR..HN.EMSC-20161027_0000016.h5	1	1		good

143	IV.T1215..HN.EMSC-20161027_0000018.h5	1	1		good
144	IV.CAFI..HN.EMSC-20161027_0000072.h5	0	0		good
145	XO.AM05..HN.EMSC-20161027_0000119.h5	1	1		good
146	3A.MZ51..HN.EMSC-20161027_0000173.h5	1	1		good
147	3A.MZ63..HN.EMSC-20161027_0000173.h5	1	1		good
148	3A.MZ24..HN.EMSC-20161027_0000177.h5	1	1		good
149	3A.MZ28..HN.EMSC-20161028_0000031.h5	1	1		good
150	3A.MZ51..HN.EMSC-20161028_0000031.h5	1	1		good
151	3A.MZ27..HN.EMSC-20161029_0000040.h5	0	0		good
152	3A.MZ19..HN.EMSC-20161029_0000048.h5	0	0		good
153	IV.MTRZ..HN.EMSC-20161030_0000029.h5	0	0		good
154	IV.ATCC..HN.EMSC-20161030_0000033.h5	1	1		good
155	IV.ATTE..HN.EMSC-20161030_0000033.h5	0	1	noisy	good
156	IV.GUMA..HN.EMSC-20161030_0000033.h5	1	1		good
157	IV.PP3..HN.EMSC-20161030_0000033.h5	1	1		good
158	IV.RM33..HN.EMSC-20161030_0000033.h5	1	1		good
159	IV.T1217..HN.EMSC-20161030_0000033.h5	1	1		good
160	IV.T1218..HN.EMSC-20161030_0000033.h5	1	1		good
161	IV.T1219..HN.EMSC-20161030_0000033.h5	1	1		good
162	IV.T1213..HN.EMSC-20161030_0000036.h5	1	1		good
163	3A.MZ19..HN.EMSC-20161030_0000037.h5	1	1		good
164	3A.MZ30..HN.EMSC-20161030_0000037.h5	1	1		good
165	3A.MZ50..HN.EMSC-20161030_0000037.h5	1	1		good
166	IV.T1201..HN.EMSC-20161030_0000037.h5	1	1		good
167	IV.T1243..HN.EMSC-20161030_0000037.h5	1	1		good
168	IV.CAFI..HN.EMSC-20161030_0000039.h5	1	1		good
169	IV.POFI..HN.EMSC-20161030_0000039.h5	1	1		good
170	IV.SNTG..HN.EMSC-20161030_0000039.h5	1	1		good
171	3A.MZ01..HN.EMSC-20161030_0000041.h5	1	1		good
172	3A.MZ11..HN.EMSC-20161030_0000041.h5	1	1		good
173	3A.MZ27..HN.EMSC-20161030_0000041.h5	1	1		good
174	3A.MZ51..HN.EMSC-20161030_0000041.h5	1	1		good
175	3A.MZ01..HN.EMSC-20161030_0000043.h5	1	1		good
176	3A.MZ28..HN.EMSC-20161030_0000043.h5	1	1		good
177	3A.MZ61..HN.EMSC-20161030_0000043.h5	1	1		good

178	3A.MZ01..HN.EMSC-20161030_0000055.h5	1	1		good
179	3A.MZ08..HN.EMSC-20161030_0000055.h5	1	1		good
180	3A.MZ29..HN.EMSC-20161030_0000055.h5	1	1		good
181	3A.MZ30..HN.EMSC-20161030_0000055.h5	1	1		good
182	3A.MZ31..HN.EMSC-20161030_0000088.h5	0	0		good
183	IV.ATLO..HN.EMSC-20161030_0000088.h5	1	1		good
184	IV.FIR..HN.IT-2012-0012.h5	1	1		good
185	IV.TERO..HN.EMSC-20101103_0000077.h5	0	1	noisy	bad
186	HP.FSK..HN.EMSC-20140507_0000022.h5	0	1	noisy	bad
187	IV.CDCA..HN.EMSC-20160530_0000085.h5	0	1	noisy	bad
188	IV.SSM1..HN.EMSC-20160824_0000006.h5	0	1	noisy	bad
189	OX.PRED..HN.EMSC-20160824_0000006.h5	0	1	noisy	bad
190	IV.MMUR..HN.EMSC-20160824_0000007.h5	0	1	noisy	bad
191	IV.ATLO..HN.EMSC-20160824_0000192.h5	0	1	noisy	bad
192	IV.CADA..HN.EMSC-20160824_0000192.h5	0	1	noisy	bad
193	IV.PP3..HN.EMSC-20160824_0000192.h5	0	1	noisy	bad
194	IV.SSM1..HN.EMSC-20161026_0000095.h5	0	1	noisy	bad
195	IV.MMUR..HN.EMSC-20161026_0000171.h5	0	1	noisy	bad
196	IV.PIEI..HN.EMSC-20161026_0000171.h5	0	1	noisy	bad
197	IV.SSM1..HN.EMSC-20161026_0000181.h5	0	1	noisy	bad
198	IV.MDAR..HN.EMSC-20161027_0000001.h5	0	1	noisy	bad
199	3A.MZ01..HN.EMSC-20161027_0000075.h5	0	1	noisy	bad
200	3A.MZ08..HN.EMSC-20161027_0000075.h5	0	1	noisy	bad
201	3A.MZ10..HN.EMSC-20161027_0000075.h5	0	1	noisy	bad
202	3A.MZ11..HN.EMSC-20161027_0000075.h5	0	1	noisy	bad
203	3A.MZ21..HN.EMSC-20161027_0000075.h5	0	1	noisy	bad
204	3A.MZ28..HN.EMSC-20161027_0000119.h5	0	1	noisy	bad
205	3A.MZ08..HN.EMSC-20161027_0000177.h5	0	1	noisy	bad
206	3A.MZ10..HN.EMSC-20161027_0000177.h5	0	1	noisy	bad
207	3A.MZ14..HN.EMSC-20161027_0000177.h5	0	1	noisy	bad
208	3A.MZ29..HN.EMSC-20161027_0000177.h5	0	1	noisy	bad
209	3A.MZ30..HN.EMSC-20161027_0000177.h5	0	1	noisy	bad
210	3A.MZ31..HN.EMSC-20161027_0000177.h5	0	1	noisy	bad
211	3A.MZ04..HN.EMSC-20161028_0000099.h5	0	1	noisy	bad

212	3A.MZ12..HN.EMSC-20161028_0000119.h5	0	1	noisy	bad
213	IV.SENI..HN.EMSC-20090407_0000144.h5	0	0		bad
214	IV.IMOL..HN.EMSC-20120529_0000138.h5	1	1		bad
215	IV.BULG..HN.EMSC-20130815_0000084.h5	1	1		bad
216	IV.EUCT..HN.EMSC-20140828_0000047.h5	1	1		bad
217	IV.IMOL..HN.EMSC-20140828_0000047.h5	1	1		bad
218	IV.ATLO..HN.EMSC-20141219_0000039.h5	1	1		bad
219	IV.IMOL..HN.EMSC-20141221_0000063.h5	1	1		bad
220	IV.INTR..HN.EMSC-20141224_0000053.h5	1	1		bad
221	IV.ZCCA..HN.EMSC-20150303_0000086.h5	0	0		bad
222	IV.BOB..HN.EMSC-20150722_0000055.h5	1	1		bad
223	IV.SBPO..HN.EMSC-20160623_0000055.h5	1	1		bad
224	IV.FIU1..HN.EMSC-20160824_0000007.h5	1	1		bad
225	IV.MDAR..HN.EMSC-20160824_0000007.h5	1	1		bad
226	IV.ATPC..HN.EMSC-20160824_0000010.h5	1	1		bad
227	IV.CERA..HN.EMSC-20160824_0000010.h5	1	1		bad
228	IV.LAV9..HN.EMSC-20160824_0000010.h5	1	1		bad
229	IV.MDAR..HN.EMSC-20160824_0000010.h5	1	1		bad
230	IV.MTL1..HN.EMSC-20160824_0000010.h5	1	1		bad
231	IV.SSFR..HN.EMSC-20160824_0000010.h5	1	1		bad
232	IV.TRIV..HN.EMSC-20160824_0000010.h5	1	1		bad
233	IV.RM33..HN.EMSC-20160824_0000011.h5	1	1		bad
234	IV.CADA..HN.EMSC-20160824_0000024.h5	1	1		bad
235	IV.FOSV..HN.EMSC-20160824_0000024.h5	1	1		bad
236	IV.NRCA..HN.EMSC-20160824_0000024.h5	1	1		bad
237	IV.PP3..HN.EMSC-20160824_0000024.h5	1	1		bad
238	IV.SSFR..HN.EMSC-20160824_0000024.h5	1	1		bad
239	IV.ATLO..HN.EMSC-20160824_0000232.h5	0	0		bad
240	IV.CAFI..HN.EMSC-20160824_0000295.h5	1	1		bad
241	IV.CPGN..HN.EMSC-20160824_0000295.h5	1	1		bad
242	IV.FIU1..HN.EMSC-20160824_0000295.h5	1	1		bad
243	IV.SSFR..HN.EMSC-20160824_0000295.h5	1	1		bad
244	XO.MN02..HN.EMSC-20160827_0000015.h5	1	1		bad

245	XO.MN02..HN.EMSC-20160827_0000071.h5	1	1		bad
246	XO.MN09..HN.EMSC-20160831_0000056.h5	1	1		bad
247	IV.ATLO..HN.EMSC-20160831_0000092.h5	0	0		bad
248	IV.NRCA..HN.EMSC-20160915_0000064.h5	1	1		bad
249	3A.MZ15..HN.EMSC-20161004_0000061.h5	1	1		bad
250	XO.AM05..HN.EMSC-20161009_0000037.h5	1	1		bad
251	3A.MZ12..HN.EMSC-20161026_0000099.h5	1	1		bad
252	3A.MZ102..HN.EMSC-20161026_0000103.h5	1	1		bad
253	3A.MZ102..HN.EMSC-20161026_0000106.h5	1	1		bad
254	3A.MZ102..HN.EMSC-20161026_0000163.h5	1	1		bad
255	3A.MZ61..HN.EMSC-20161027_0000032.h5	1	1		bad
256	3A.MZ102..HN.EMSC-20161027_0000059.h5	1	1		bad
257	3A.MZ04..HN.EMSC-20161027_0000075.h5	1	1		bad
258	3A.MZ50..HN.EMSC-20161027_0000075.h5	1	1		bad
259	3A.MZ51..HN.EMSC-20161027_0000075.h5	1	1		bad
260	3A.MZ31..HN.EMSC-20161027_0000119.h5	1	1		bad
261	3A.MZ51..HN.EMSC-20161027_0000119.h5	1	1		bad
262	3A.MZ102..HN.EMSC-20161027_0000121.h5	1	1		bad
263	3A.MZ11..HN.EMSC-20161027_0000177.h5	1	1		bad
264	3A.MZ12..HN.EMSC-20161027_0000177.h5	1	1		bad
265	3A.MZ10..HN.EMSC-20161028_0000031.h5	1	1		bad
266	3A.MZ102..HN.EMSC-20161028_0000031.h5	1	1		bad
267	3A.MZ11..HN.EMSC-20161028_0000031.h5	1	1		bad
268	3A.MZ12..HN.EMSC-20161028_0000031.h5	1	1		bad
269	3A.MZ19..HN.EMSC-20161028_0000031.h5	1	1		bad
270	3A.MZ21..HN.EMSC-20161028_0000031.h5	1	1		bad
271	3A.MZ24..HN.EMSC-20161028_0000031.h5	1	1		bad
272	3A.MZ26..HN.EMSC-20161028_0000031.h5	1	1		bad
273	3A.MZ29..HN.EMSC-20161028_0000031.h5	1	1		bad
274	3A.MZ31..HN.EMSC-20161028_0000031.h5	1	1		bad
275	3A.MZ61..HN.EMSC-20161028_0000031.h5	1	1		bad
276	3A.MZ11..HN.EMSC-20161028_0000099.h5	0	0		bad
277	3A.MZ12..HN.EMSC-20161028_0000099.h5	1	1		bad

278	3A.MZ14..HN.EMSC-20161028_0000099.h5	1	1		bad
279	3A.MZ26..HN.EMSC-20161029_0000040.h5	1	1		bad

Data and Resources

The documentation of the ar_pick algorithm in Obspy is available at https://docs.obspy.org/packages/autogen/obspy.signal.trigger.ar_pick.html, whereas the documentation of the recursive STA/LTA trigger algorithm in Obspy is available at https://docs.obspy.org/packages/autogen/obspy.signal.trigger.recursive_sta_lta_py.html.

References

Akazawa, T. (2004). A technique for automatic detection of onset time of P-and S-Phases in strong motion records, 13th World Conference on Earthquake Engineering.

Puglia, R., E. Russo, L. Luzi, M. D’Amico, C. Felicetta, F. Pacor, and G. Lanzano (2018). Strong motion processing service: A tool to access and analyze earthquakes strong motion waveforms, Bull. Earthq. Eng. 16, 2641–2651.

Trnkoczy, A., P. Bormann, W. Hanka, L.G. Holcomb, and R.L., Nigbor (2012). Site selection, preparation and installation of seismic stations. In New Manual of Seismological Observatory Practice 2 (NMSOP-2) (pp. 1-139). Deutsches GeoForschungsZentrum GFZ.